INVESTIGATION OF THE CONDENSATION SHOCK IN AIR BY USE OF THE SCHLIEREN METHOD

WALDO WATSON SIMONS
JOHN SARTOR BOWEN

COPY FOR HEAD OF POSTGRADUATE SCHOOL

MASSACHUSETTS INSTITUTE OF TECHNOLOGY
Department of Mechanical Engineering
Cambridge 39, Mass., U.S.A.

Room 5-202

September 24, 1946

Captain W. R. Bura[illegible]
Room 5-233
Massachusetts Institute of Technology
Cambridge 39, Massachusetts

Thesis Work of LT E. L. PERRY, USCG
LT L. W. A. RENSHAW, USCG
LCDR W. W. SIMONS, USN
LCDR J. S. BOWEN, USN

Dear Captain Buracker:

The thesis by Lieutenants E. L. Perry and L. W. A. Renshaw entitled "Schlieren Observation of Supersonic Discharge" presents pressure measurements and Schlieren photographs of supersonic streams discharging into an exhaust space under various conditions. The photographs show interesting detail which in general corresponds to analytical results. The most significant observation was a comparison of two supersonic streams alike in average conditions but differing in the thickness of the boundary layer. The effect of boundary-layer thickness on the nature of the shock pattern is shown clearly.

The thesis by Lt. Comdrs. W. W. Simons and J. S. Bowen entitled "Investigation of the Condensation Shock in Air by Use of the Schlieren Method" presents pressure measurements and Schlieren photographs of the shock patterns when water vapor in air condenses to form a fog of liquid or solid particles. It has extended our knowledge of the conditions which control condensation and of the condensation shock which accompanies it.

From either of these theses a paper could be prepared which would be published in one of the journals of the professional societies.

Yours truly,

/s/ Joseph H. Keenan

Joseph H. Keenan

INVESTIGATION OF THE CONDENSATION SHOCK IN AIR BY USE OF THE SCHLIEREN METHOD

By

Waldo W. Simons, Lieut. Commander, U.S. Navy
S.B., U.S.Naval Academy, 1941

John S. Bowen, Lieut. Commander, U.S. Navy
S.B., U.S.Naval Academy, 1941

SUBMITTED IN PARTIAL FULFILLMENT OF THE REQUIREMENTS FOR THE DEGREE OF MASTER OF SCIENCE

at the
MASSACHUSETTS INSTITUTE OF TECHNOLOGY
1946

MASSACHUSETTS INSTITUTE OF TECHNOLOGY
77 Massachusetts Avenue
Cambridge, Massachusetts

September 16, 1946

Professor J. S. Newell
Secretary of the Faculty
Massachusetts Institute of Technology
77 Massachusetts Avenue
Cambridge, Massachusetts

Dear Professor Newell:

Herewith we submit our thesis entitled "Investigation of the Condensation Shock in Air by use of the Schlieren Method" in partial fulfillment of the requirements for the Degree of Master of Science in Naval Construction and Engineering at the Massachusetts Institute of Technology.

Very truly yours,

ACKNOWLEDGEMENT

We acknowledge with pleasure our indebtedness to Professor J. H. Keenan for his suggestion of the thesis topic and method of attack. Professor E. P. Neumann and Professor A. H. Shapiro gave freely of their time in guiding the progress of our investigation.

TABLE OF CONTENTS

		Page
	Index of Tables and Figures	
I.	Summary	1
II.	Introduction	3
III.	Procedure	5
IV.	Table of Symbols	9
V.	Results	11
VI.	Discussion of Results	32
VII.	Recommendations	49
VIII.	Appendix	50
IX.	Bibliography	64

INDEX OF TABLES AND FIGURES

		Page
Table I	- Data for Figures V, VI and VII	23
Table II	- $T_{sat} - T_1$	43
Table III	- Original Data	51
Table IV	- Original Data	56
Table V	- Original Data	58
Table VI	- Data of nozzle areas and area ratios	59
Table VII	- Detailed calculation across the condensation shock	61
Table VIII	- Drop size calculation	62
Figure I	- Schematic Diagram of Apparatus	7
Figure II	- Location of Pressure Taps and Reference Lines	8
Figure III	- Position of shock Vs relative humidity	21
Figure IV	- Position of shock Vs specific humidity	22
Figure V	- $\frac{P}{P_o}$ Vs distance along the nozzle	25
Figure VI	- " " " " " "	26
Figure VII	- " " " " " "	27
Figure VIII	- $\frac{P_2 - P_1}{P_o}$ Vs specific humidity	28
Figure IX	- A_1/A_T " " "	33
Figure X	- W_2/W_1 Vs W_1	41
Figure XI	- T_{sat} Vs specific humidity	44
Figure XII	- Saturation pressures for various drop sizes	47
Figure XIII	- Area and area ratio Vs distance along the nozzle	60

SUMMARY

The object of this investigation is to study the effect of variation of moisture content in air upon the formation of a condensation shock. An ejector was used to draw air through a two dimensional converging-diverging nozzle with glass walls. Moisture content of the air was varied by a dehumidifier. Schlieren pictures of the flow were taken from which measurements of the position of the shock were made. Also pressure measurements were taken along the nozzle. The humidity of the inlet air was measured with wet and dry bulb thermometers.

The results obtained by correlation of the data for a nozzle of constant angle of divergence are:

(1) The pressure rise due to a condensation shock is a direct function of the specific humidity of the inlet air. (Figure VIII).

(2) For a given inlet temperature, the distance of the condensation shock downstream of the throat varies inversely as the specific humidity of the air. (Figure IV). From this relation, it is postulated that the position of the area ratio at which the shock would occur can be plotted against specific humidity for a given inlet temperature. In this way, the curve will

serve for nozzles of various contours. (Figure IX).

(3) The amount of water vapor condensing out in the condensation shock can be predicted if the inlet specific humidity is known (Figure X).

(4) The difference between the temperature at which the water vapor becomes saturated under equilibruim conditions and the temperature at which the condensation shock occurs, as the humid air passes through the nozzle, is essentially a constant of about 110° F.

(5) The drop size of the water condensing out in the shock is essentially a constant. This is shown on Figure XII.

INTRODUCTION

When humid air is expanded by passage through a simple convergent-divergent nozzle, the water vapor remains a vapor at the saturation temperature and below and continues to expand into the supersaturated region. Part of the water vapor in this meta-stable state condenses out rapidly at a certain point along the nozzle. At the point of condensation a pressure rise occurs in the stream. This phenomena is known as the condensation shock.

A more complete understanding of the condensation shock is necessary at the present time due to recent increase of flow speeds into the supersonic region. Difficulty has been experienced in the design of supersonic wind tunnels and in gas turbine research due to the presence of condensation shocks.

Very little information on the condensation shock is available in the literature at present. J. I. Yellott and C. K. Holland (1)* (2)* have investigated the condensation shock in steam. R. Hermann (3) in 1934-36 studied the condensation shock in air. These experiments were primarily designed for the provision of data in connection with the construction of a workable supersonic wind tunnel. Hermann verified previous experiments by showing

* (1) (2) Refer to numbered references in the Bibliography page 64.

that there is a unique position of the shock in the nozzle depending upon the relative humidity of the air. K. Oswatitsch (4) published in 1942 a step by step method of computing the pressure as a function of distance along a nozzle in the region of the condensation shock. This method was applied to measured data of Yellott and Holland and A.M. Binnie and M.W. Woods (5), and his own experimental data, and excellent correlation was obtained. As mentioned, however, the experimental data in this field is small, and the purpose of our study is to verify previous results and obtain additional information on the laws governing the condensation shock.

PROCEDURE AND DESCRIPTION OF APPARATUS

The Schlieren apparatus is an optical method of indicating density gradients of the flow in a nozzle. This apparatus is adequately described in reference (6), pp. 26-28 and pp. 33-38. In order to stop any possible movement of the shock, the Edgerton High Speed Flash Unit, reference (6), pp. 39-42, was used. The indicated flash duration of one-five millionths of a second is not attained due to stray wire capacitance, but the unit provides sufficient speed for the purposes of this study.

A steam ejector was used to maintain a vacuum of about 27 inches of Hg. on the nozzle exhaust. This insured supersonic flow in the nozzle. A schematic diagram of the apparatus is shown in Figure I. Atmospheric air may be drawn through valve B and dehumidified air through valve A. By adjustment of valves A and B, the relative humidity of the air can be varied about 40%. The maximum pressure drop through the dehumidifier was 1.5 cm. of Hg.

Humidity measurement was made by means of a wet and dry bulb thermometer at the nozzle inlet. Paired, rapid reading thermometers were used.

As shown in Figure II, reference lines were placed

at the throat and at a station 3.2 inches below the throat. This enabled us to accurately measure the position of the shock and also to determine the foreshortening of the photograph taken. Pressure taps were placed along the nozzle at points indicated. Pressures were measured by mercury manometers. An additional pressure tap was located in the 2" nozzle inlet pipe.

Simultaneous readings of pressures and of wet and dry bulb thermometers were made after a steady state of flow was obtained for the desired relative humidity. Either a picture was taken or the position of the shock measured directly from the camera screen.

FIGURE I

DIAGRAMMATIC SKETCH OF APPARATUS

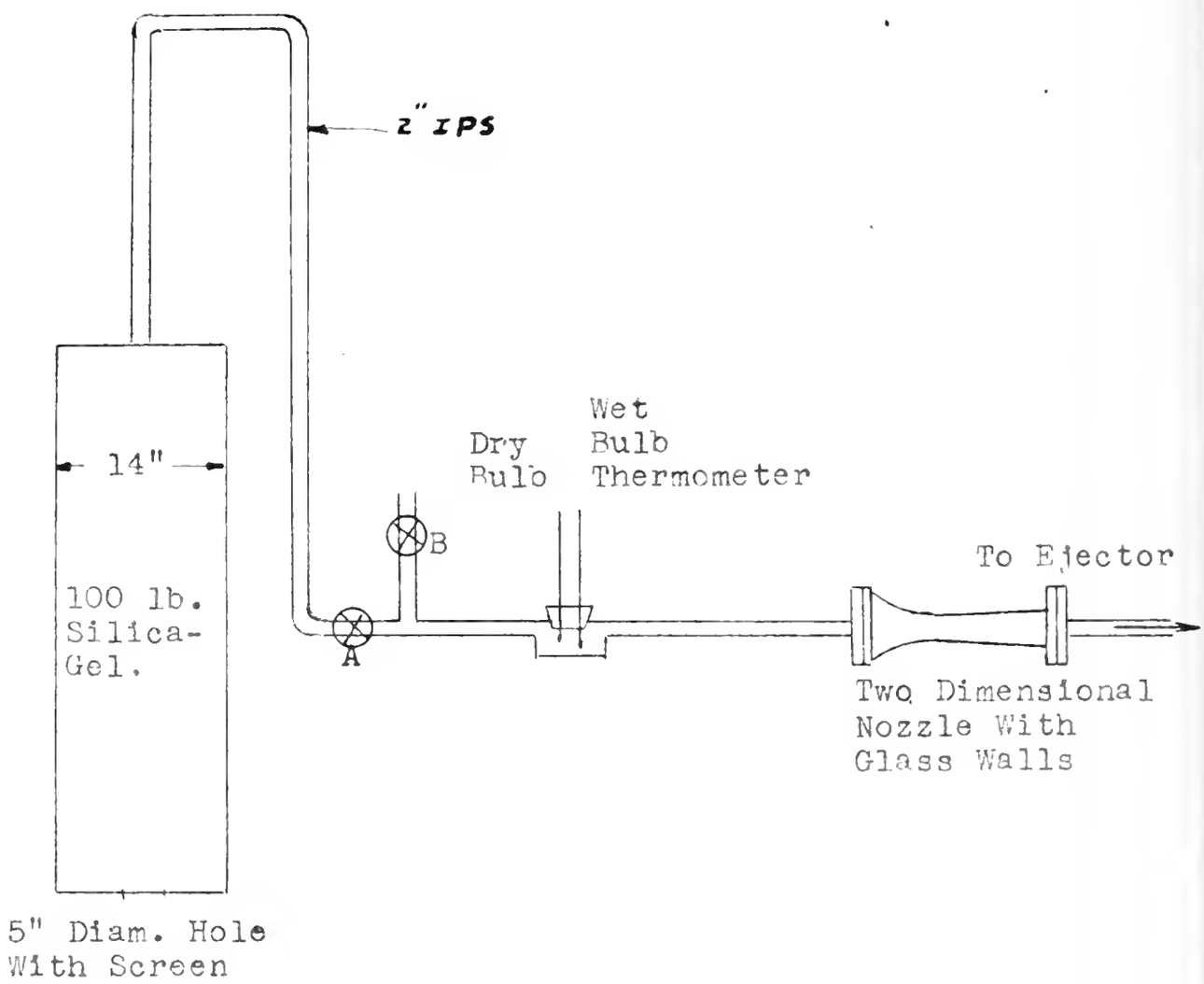

LOCATION OF PRESSURE TAPS AND REFERENCE LINES ON NOZZLE

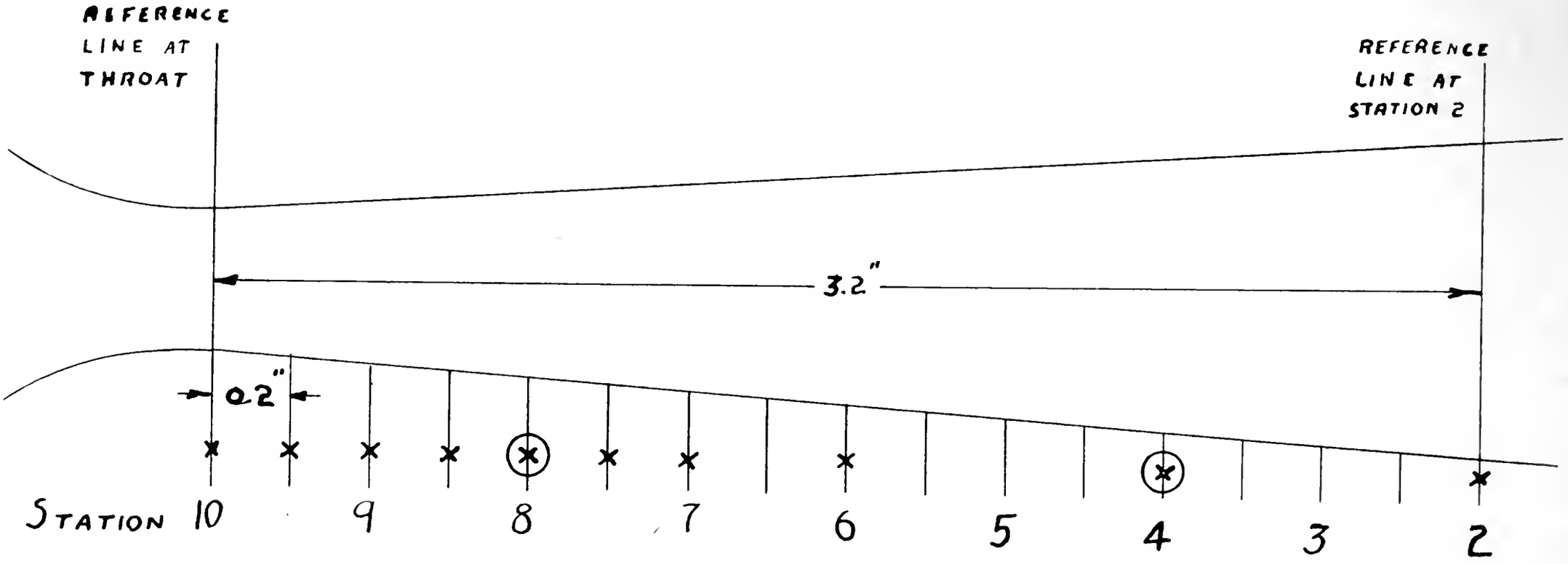

× PRESSURE TAP LOCATION

⊗ PRESSURE TAPS FROM WHICH MEASUREMENTS REJECTED

FIGURE II

TABLE OF SYMBOLS

A	- Area, ft.^{2}
c_{p_a}	- Specific heat at constant pressure of air, 0.24 B.T.U./lb. $^\circ$F
$c_{p_{wv}}$	- Specific heat at constant pressure of water vapor, at low pressure, 0.44 B.T.U./lb. $^\circ$F
g	- Acceleration of gravity, 32.2 ft./sec.^{2}
H	- Enthalpy of a mixture of air and water vapor (plus ice or water if appropriate) B.T.U./lb.
h_a	- Enthalpy of air, B.T.U./lb.
h_i	- Enthalpy of ice, B.T.U./lb.
h_{wv}	- Enthalpy of water vapor, B.T.U./lb.
h^*	- Heat of vaporization or sublimation, B.T.U./lb.
J	- Mechanical equivalent of heat, 778 ft. lbs/B.T.U.
k	- Isentropic exponent for the mixture, taken as 1.4
M	- Mach No.
m_a	- Lbs. of air
m_{wv}	- Lbs. of water vapor
m^*	- Lbs. of water or ice condensing out in the condensation shock
P	- Pressure of the mixture, lbs./in.^{2}
P_s	- Partial pressure of the water vapor, lbs./in.^{2}
P_a	- Partial pressure of the air, lbs./in.^{2}
$P_{s\infty}$	- Saturation pressure for water vapor in thermal equilibrium with drops of infinite radius, lbs./in.^{2}
P_{sr}	- Saturation pressure for water vapor in thermal equilibrium with drops of radius r, lbs./in.^{2}
r	- Radius of water droplets, ft.

t - Temperature, ^{o}F

T - Temperature, ^{o}F absolute

T_{sat} - Temperature at which the water vapor in the air becomes saturated, considering a stable state exists, as humid air flows through the nozzle, ^{o}F absolute

V - Velocity, ft./sec.

v - Specific volume of the mixture, $ft.^3/lb.$

v^i - Specific volume of water at the temperature of a drop, $ft.^3/lb.$

w or ω - Specific humidity, lbs. of water vapor per lb. of air

x - Actual distance from throat to condensation shock

x^* - Distance from throat to condensation shock as measured on a picture

σ - Surface tension of water, lbs./ft.

ϕ - Relative humidity

Subscripts

No subscript - Any position in the nozzle

0 - State at nozzle entrance

1 - State at an infinitesimal distance before the shock

2 - State at an infinitesimal distance after the shock

a - Air

wv - Water vapor

RESULTS

The data of tables III, IV & V (see Appendix) was obtained in sequence. Table III gives the results of two sets of runs taken on two different days and is arranged in order of decreasing relative humidity. High humidity runs 1, 2, 3, and 4 were obtained using steam to humidify the air. The pictures for these give qualitative results but the data is considered questionable. The pictures obtained during these runs follow and are arranged in order of decreasing specific humidity.

Upon reviewing the above data, it was considered desirable to obtain more pressure data in the vicinity of the shock. Additional pressure taps were added (see Figure II). Table IV presents the results obtained. Pressure measurements were taken but no additional pictures. Pressures at stations 8 and 4 were unreliable due to oblique shocks originating at their pressure taps.

Upon making the plot of x/t (defined on figures III and IV) Vs specific humidity, shown in Figure IV, it was believed that x/t was a straight line function of specific humidity for a given inlet temperature. The data of Table V presents additional information for a lower range of inlet temperatures than had been obtained previously. Pictures were not taken but

values of x were measured directly from the camera screen.

PICTURES

The pictures of runs 1, 2, and 3 are taken with dark field and the condensation shock appears light. All other pictures are taken with light field and the condensation shock shows up as a dark band. Steam was used to increase the humidity of runs 1, , 3 and 4. x^* is the distance from the throat to the condensation shock as measured on the picture. The actual distance from the throat to the condensation shock = $x = x^*$ (1.07).

Run 1, ϕ = 100%, x^* = 0.34 in.

Run 2, ϕ = 86.8%, w = 0.02118, x^* = 0.33 in.

Run 4, ϕ = 7 3%, w = 0.0171, x^* = 0.39 in.

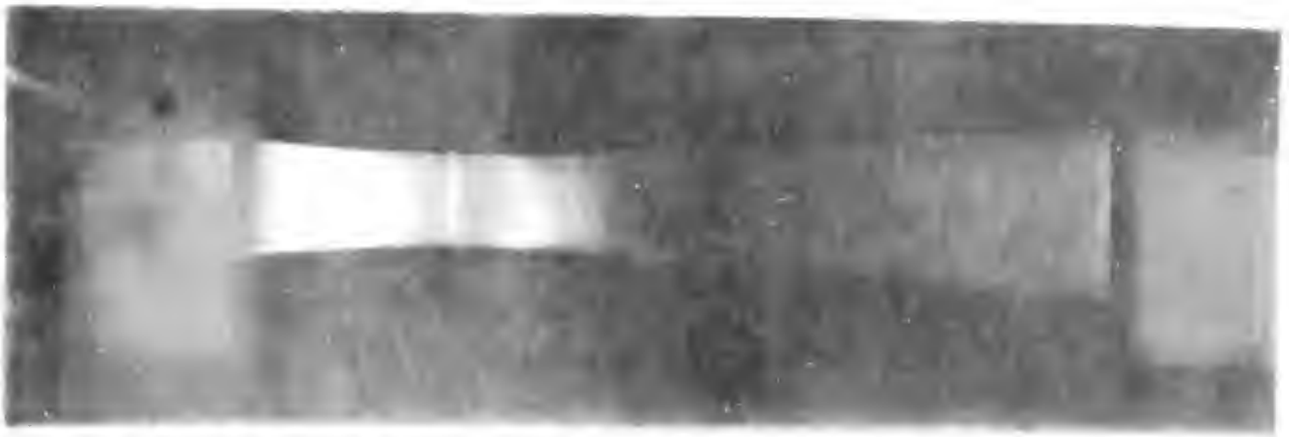

Run 3, ϕ = 77%, w = 0.0170, x^* = 0.35 in.

Run 8, ϕ = 56%, w = 0.01439, x^* = 0.49 in.

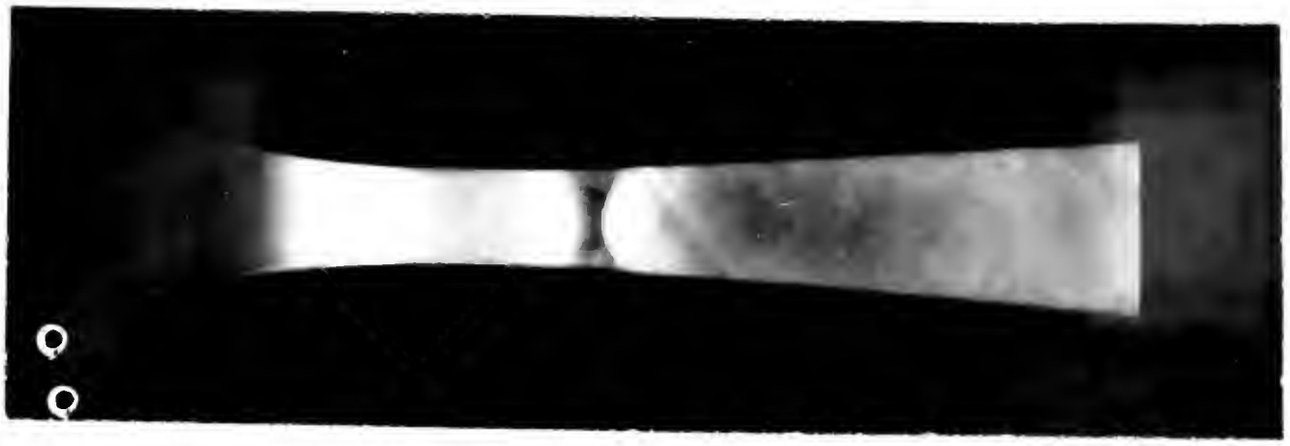

Run 9, ϕ = 51%, w = 0.01528, x^* = 0.53 in.

Run 6, ϕ = 33%, w = 0.01313, x^* = 0.47 in.

Run 12, ϕ = 17%, w = 0.01205, x^* = 0.55 in.

Run 15, ϕ = 45.6%, w = 0.01190, x^* = 0.30 in.

Run 16, ϕ = 42%, w = 0.01092, x^* = 0.00 in.

Run 18, ϕ = 51%, w = 0.01070, x^* = 0.57 in.

Run 20, ϕ = 5[illegible], w = 0.01027, x^* = 0.65 in.

Run 17, ϕ = 42%, w = 0.01011, x^* = 0.55 in.

Run 18, ϕ = 4 %, w = 0. 1014, x^* = 0.56 in.

Run 15, ϕ = 46%, w = 0.00992, x^* = 0.52 in.

Run 22, ϕ = 36%, w = 0.00982, x^* = 0.35 in.

Run 23, ϕ = 54%, w = 0.00964, x^* = 0.35 in.

Run 21, ϕ = 17%, w = 0.00981, x^* = 0.35 in.

Run 24, ϕ = 30.5°, w = 0.00813, x^* = 0.76 in.

Run 25, ϕ = 27.5°, w = 0.00756, x^* = 0.80 in.

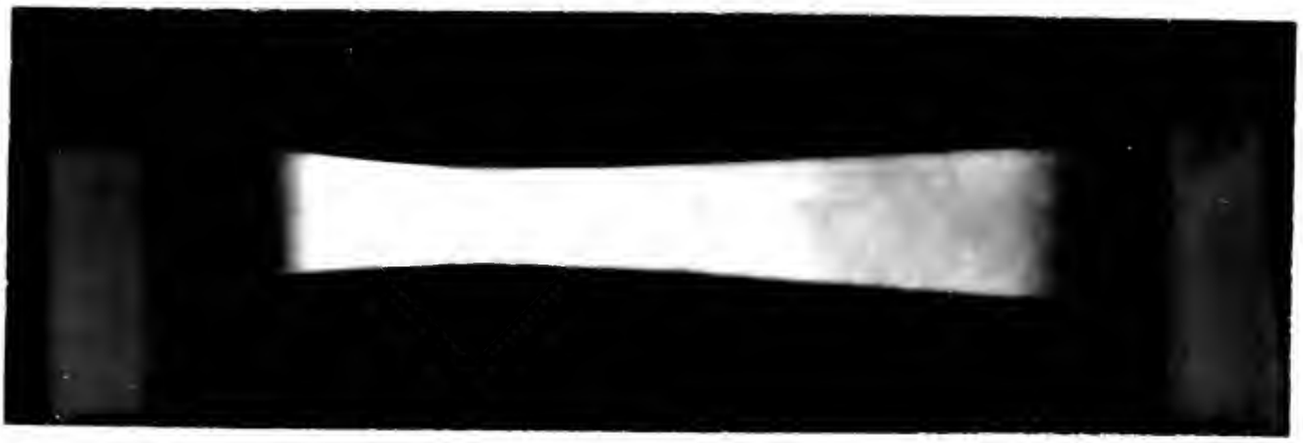

Run [illegible], ϕ = 22°, w = 0.00741, x^* = 0.88 in.

Figure III shows a plot of the dimensionless ratio x/t Vs relative humidity. This plot shows the same trend as a similar plot of R. Hermann (3). Relative humidity is not an absolute quantity. Therefore this plot represents qualitative results only.

It was decided to use specific humidity as a parameter since this is an absolute quantity. Specific humidity, w, is defined as lbs. of water vapor per lb. of air. Figure IV shows a plot of x/t Vs specific humidity. The inlet temperature of the air for each point is indicated on the figure. It appears from Figure IV that x/t is a straight line function of w for a given inlet temperature.

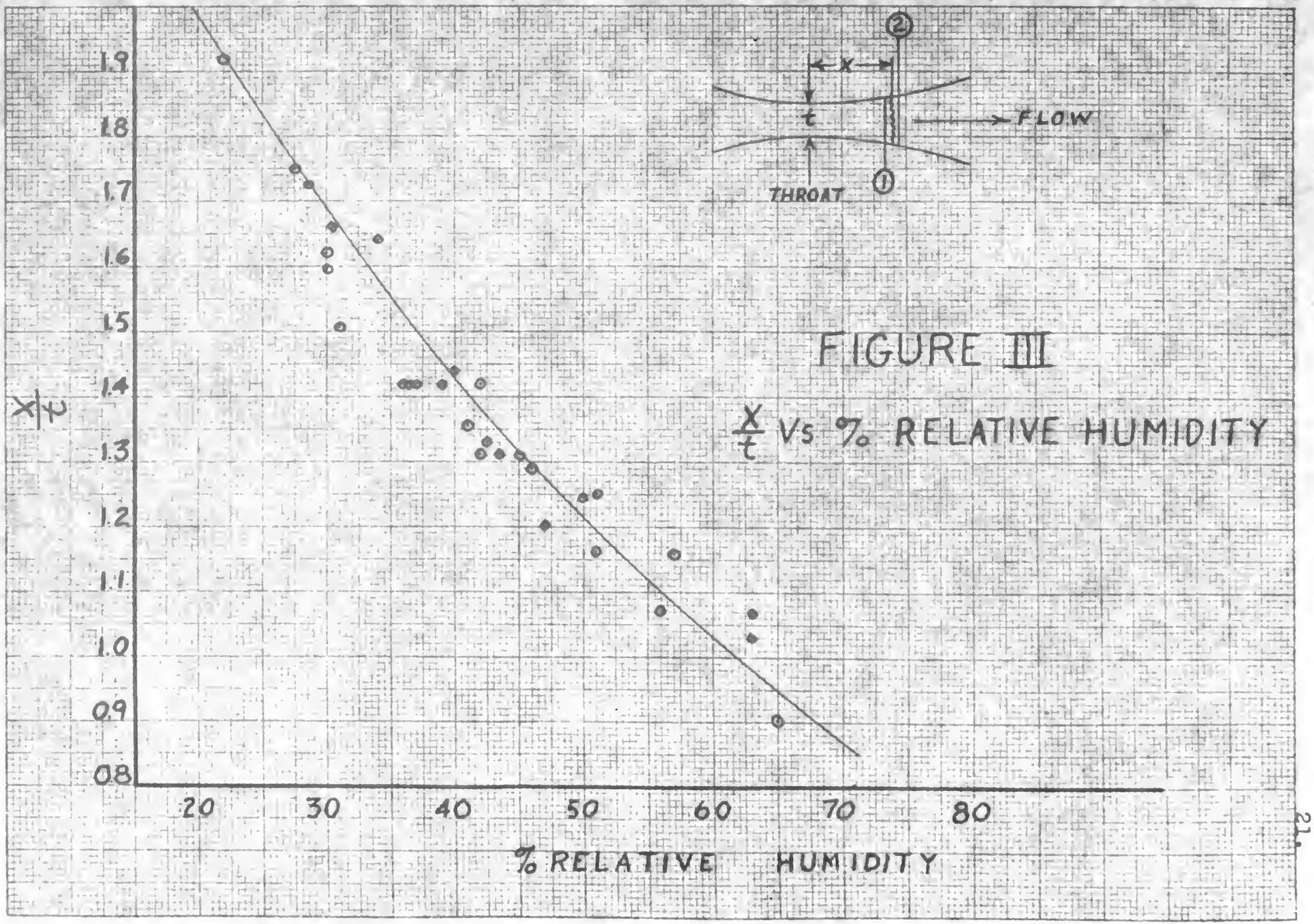

FIGURE III

$\frac{X}{t}$ Vs % RELATIVE HUMIDITY

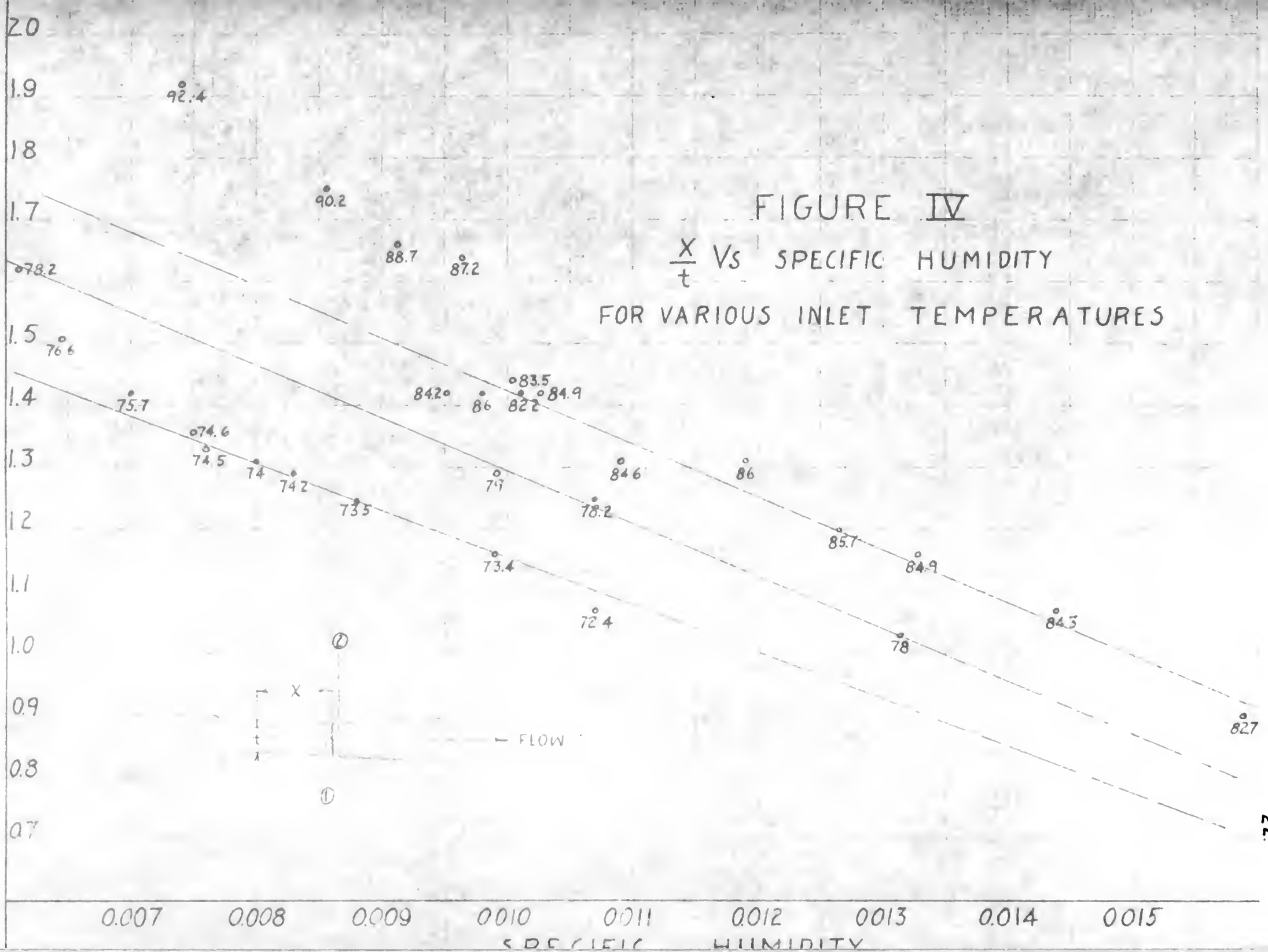

FIGURE IV

$\frac{X}{t}$ Vs SPECIFIC HUMIDITY

FOR VARIOUS INLET TEMPERATURES

Data for plotting curves 1 to 8 on Figures V, VI, and VII was obtained as indicated in the following table.

TABLE I

Curve	Run	Table	ω	$\omega_{Av.}$	$(P_2-P_1)/P_o$	X	Symbol
1	1	II	.00581	.00581	0.044	0.83	⊡
2	2	II	.00714	.00714	0.051	0.81	△
3	4	II	.00997				⊡
	19	I	.00975	.00985	0.062	0.70	⊙
	22	I	.00982				△
4	5	II	.01082	.01087	0.073	0.65	⊡
	16	I	.01092				⊙
5	6	II	.01254	.01259	0.092	0.59	×
	12	I	.01265				▽
6	8	II	.01358	.01343	0.094	0.55	▽
	9	I	.01328				+
7	9	II	.01384	.013814	0.082	0.515	×
8	5	I	.01588	.01588	0.106	0.43	⊙

As shown in the table, runs with about the same specific humidity and inlet temperature were grouped, where possible, to correlate the data.

These curves were plotted to represent an instantaneous pressure rise at the position of the shock as defined below:

(1) The pressure ratios P/P_o, from the throat down to the location of the shock were plotted against distance along the nozzle.

(2) Pressure ratios downstream of the shock were plotted.

(3) These curves were extrapolated to the location of the shock as determined from the photographs taken.

(4) The vertical distance between the two curves was taken to represent an equivalent pressure rise which could be used to represent the condensation shock in calculations. This is the value $(P_2-P_1)/P_o$.

Curve VIII shows $\frac{P_2-P_1}{P_o}$ Vs specific humidity. This curve shows that the pressure rise in a nozzle is a direct function of specific humidity.

Before proceeding with the discussion of the results, the limitation on accuracy of the data presented must be mentioned. Steady state conditions for any one run were difficult to obtain, but relative humidity never varied over 0.5%. This variation resulted from the rise of inlet temperature caused by the dehydrating action of the silica-gel. Because the pressure measurement showed no variation over the duration of a run, it is

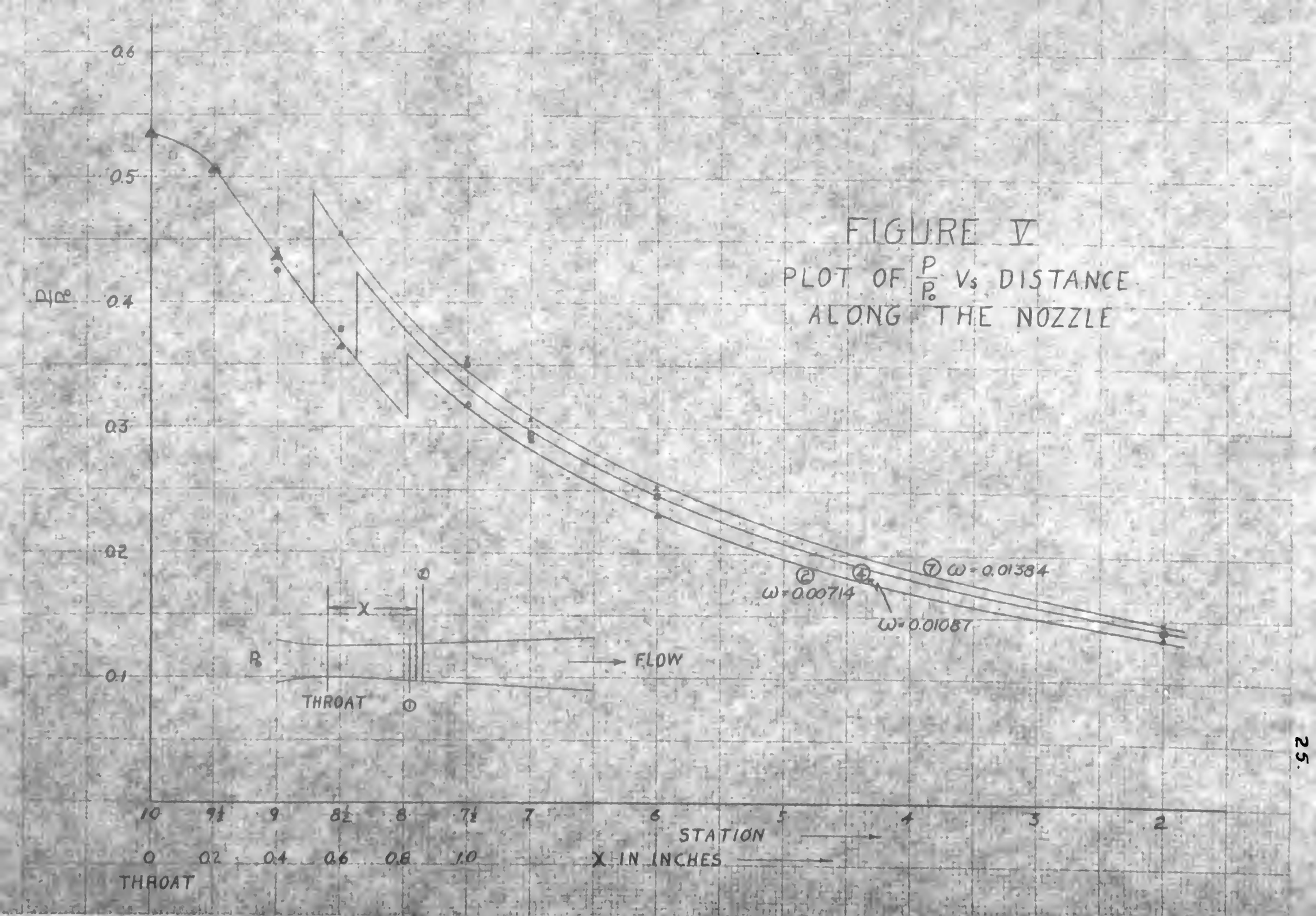
FIGURE V
PLOT OF P/P₀ Vs DISTANCE ALONG THE NOZZLE
P/P₀
0.6
0.5
0.4
0.3
0.2
0.1
② ω = 0.00714
④
⑦ ω = 0.01384
ω = 0.01087
X
D
R
FLOW
THROAT
①
10
9½
9
8½
8
7½
7
6
5
4
3
2
STATION
0
0.2
0.4
0.6
0.8
1.0
X IN INCHES
THROAT

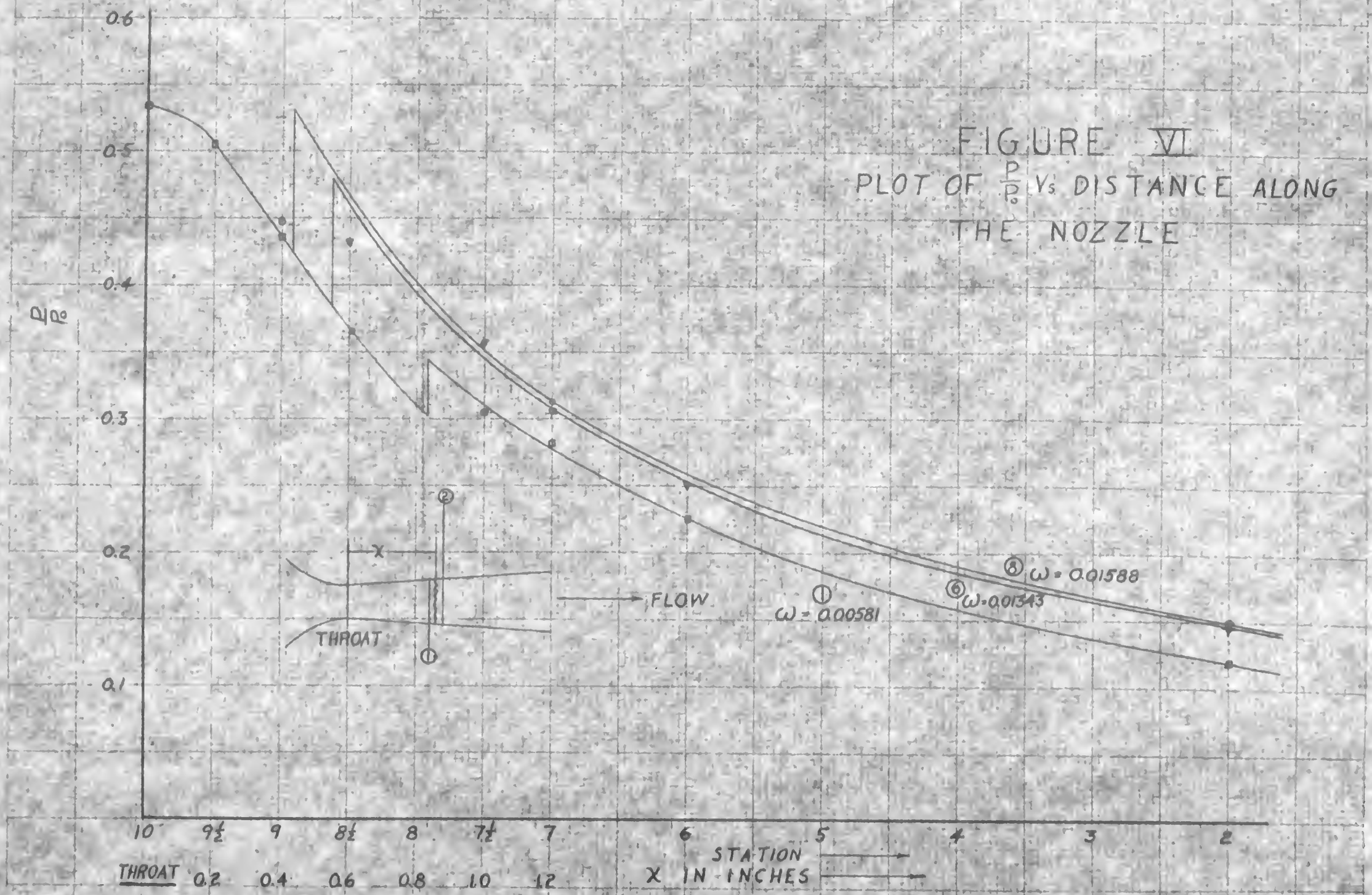

FIGURE VI

PLOT OF $\frac{P}{P_o}$ Vs DISTANCE ALONG THE NOZZLE

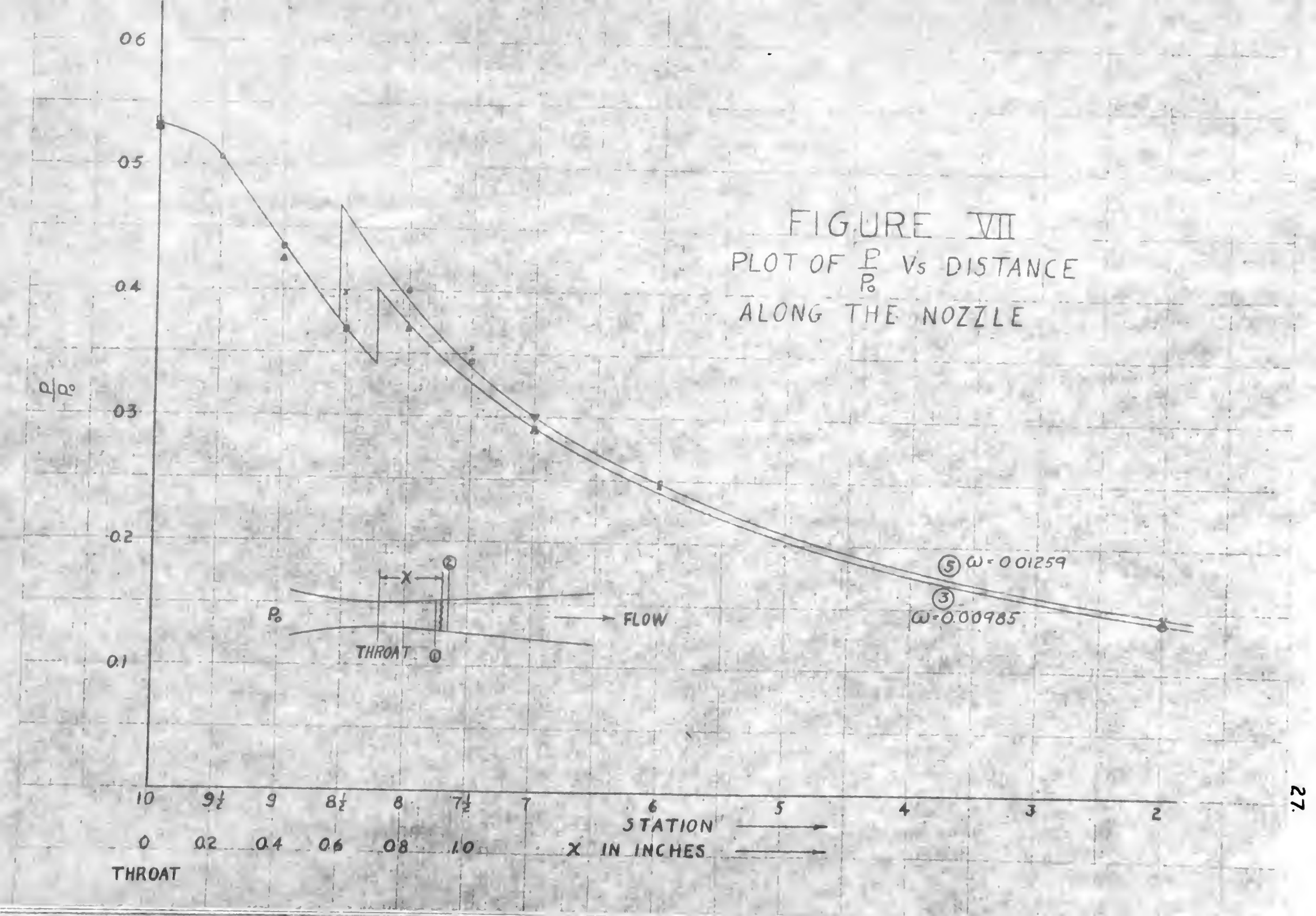
FIGURE VII
PLOT OF P/P₀ Vs DISTANCE
ALONG THE NOZZLE
P/P₀
0.6
0.5
0.4
0.3
0.2
0.1
⑤ ω = 0.01259
③ ω = 0.00985
P₀
X
②
①
THROAT
FLOW
10
9½
9
8½
8
7½
7
6
5
4
3
2
STATION
X IN INCHES
0
0.2
0.4
0.6
0.8
1.0
THROAT

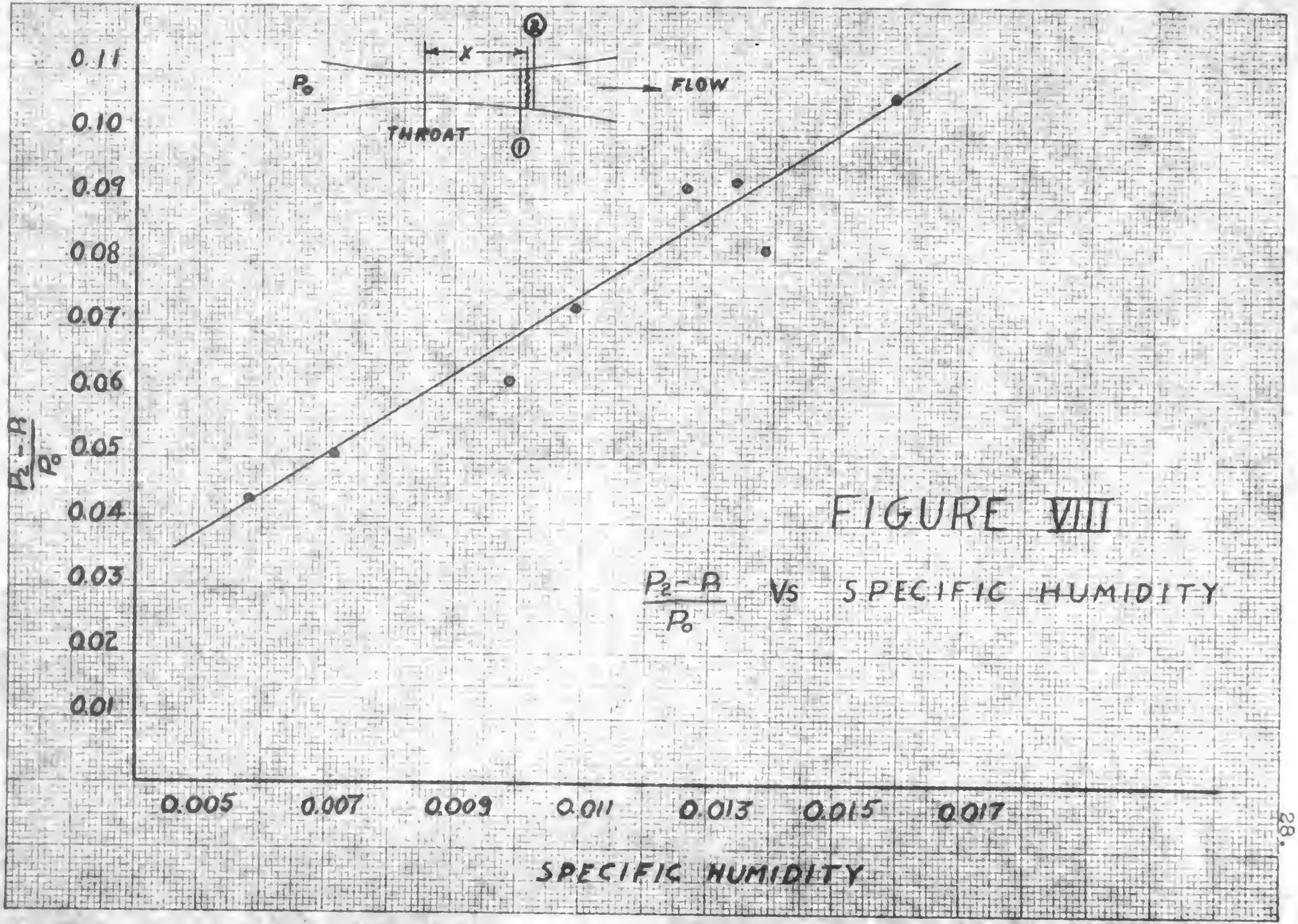

FIGURE VIII

$\frac{P_2 - P}{P_0}$ Vs SPECIFIC HUMIDITY

felt that the specific humidity remained essentially constant.

Quick reading, large scale, paired thermometers were used in humidity measurements. Air passed over wet and dry bulbs at 3,000 ft./min. which is well over the 600 ft./min. minimum velocity required. Relative humidity was obtained by means of reference (9).

Specific humidity was read from Table VII or Chart XII of reference (8). The accuracy of the recorded specific humidity was about ± 0.00005 lbs. water vapor/lb. air.

Measurements of x^*, the distance of the shock downstream of the throat, were measured to the center of the shock to an accuracy of about ± 0.01 inch. These distances had to be corrected for foreshortening. The two reference lines placed 3.2 inches apart on the nozzle measured 2.99 inches on the pictures, giving a correction factor of $\frac{3.2}{2.99}$ or 1.07 which has to be applied to measurements taken from pictures.

Due to the physical nature of the condensation shock which occurs over a relatively broad area, the measurements were made to the point of maximum density as mentioned above. It may be shown by comparisons of pictures A and B how sensitivity in adjustment of the

Schlieren Apparatus can vary the apparent width of the condensation shock. The condensation shock may be represented as shown below.

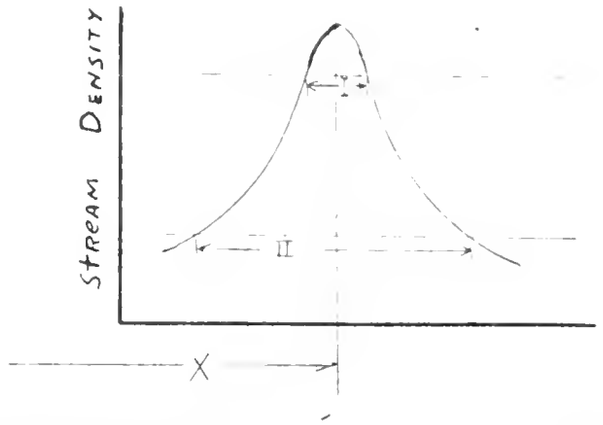

Low Sensitivity Picture A, Shock of apparent width I

High Sensitivity Picture B, Shock of apparent width II

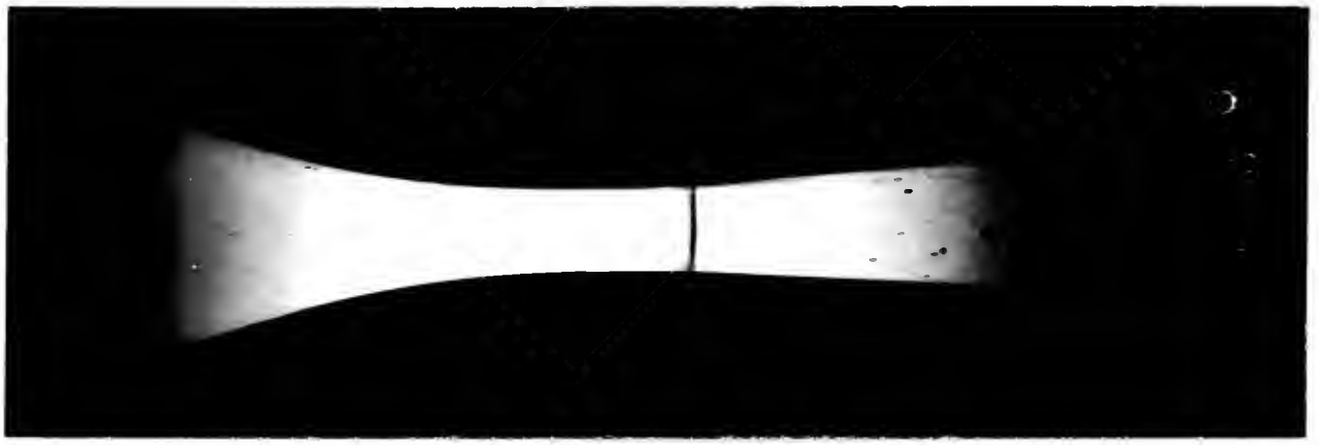

Picture A, ω = 0.0168, Low sensitivity adjustment

Picture B, ω = .01788, High sensitivity adjustment

The pressure measurements obtained are considered accurate to ± 0.5 mm. Hg. Oblique shocks, observed on the pictures, from Stations 8 and 4 were believed to have resulted in unreliable readings and the pressure readings at these stations were not used.

Upon measuring the areas of the nozzle contour, it was found that the measured areas did not agree with the nozzle design. Nozzle area measurements were made by micrometer to an accuracy of .001 inch. The results of these measurements are listed on Table VI in the Appendix. A plot of area and area ratio Vs distance along the nozzle (Figure XIII) follows Table VI.

DISCUSSION OF RESULTS

As brought out in the RESULTS, the following correlations were obtained for the test nozzle.

(1) For a given relative humidity, the location of the shock can be predicted within narrow limits.

(2) For a given inlet temperature and specific humidity, the location of the shock can be predicted.

(3) For a given specific humidity, the pressure rise across the shock can be predicted.

In order that the information of Figure IV may be of use for nozzles of various designs, Figure IX has been prepared. This figure shows area ratio Vs specific humidity, where area ratio is the ratio of the area at the position of the shock to the nozzle throat area. It is proposed that the results of Figure IX will hold for nozzles of various contours.

The results and conclusions stated to this point have been derived directly from the experimental data. It is now proposed to investigate the mechanism of the condensation shock by analytical methods. In particular, the following conclusions will be brought out:

(1) For a given specific humidity, the amount of moisture condensing out at the position of the shock will be predicted.

FIGURE IX

$\frac{A}{A_T}$ Vs SPECIFIC HUMIDITY

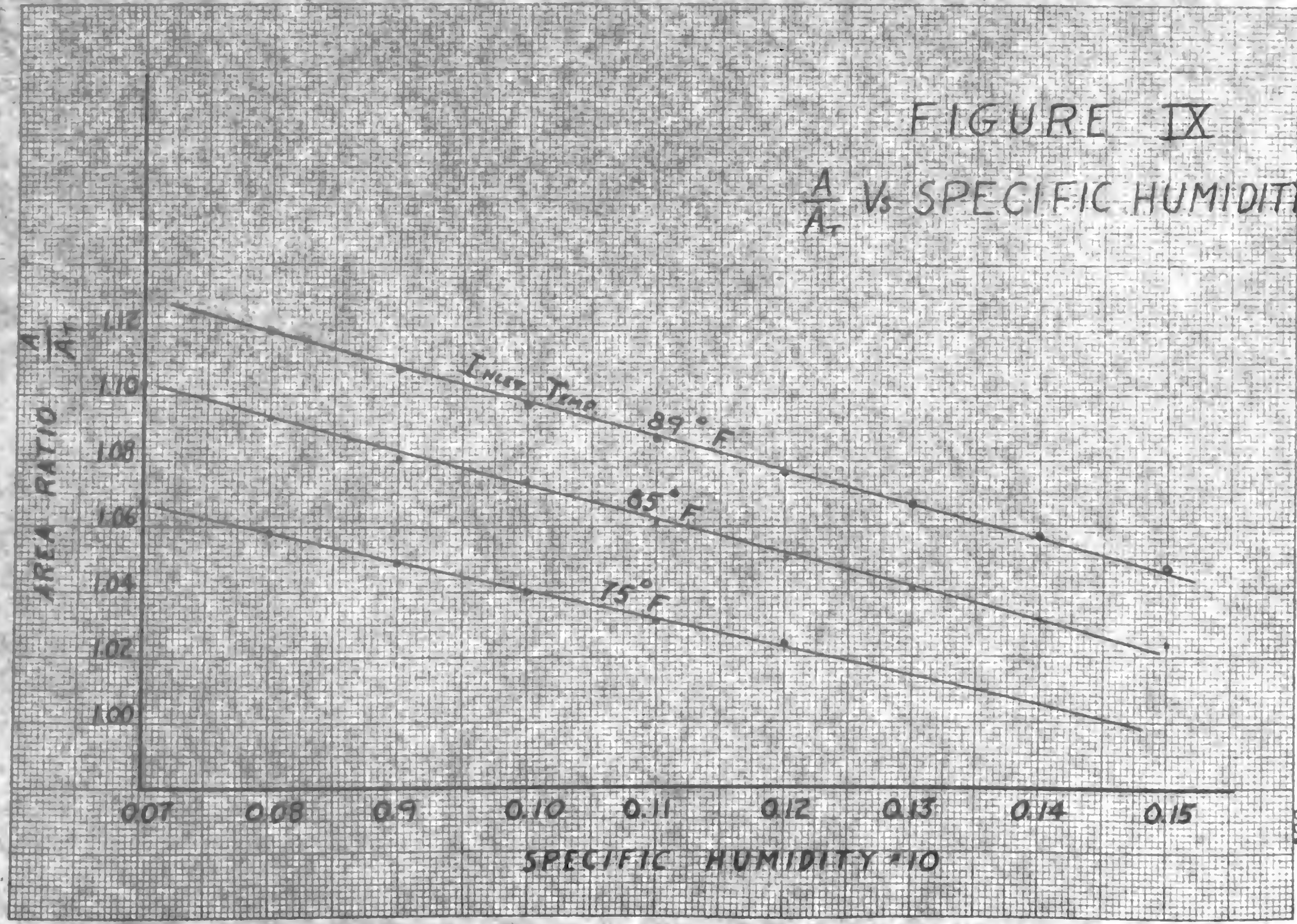

(2) For any specific humidity and inlet temperature, it will be shown that the difference between the temperature at which the air becomes saturated under equilibrium conditions and the temperature at which condensation occurs is essentially a constant. ($T_{sat}-T_1$).

(3) The order of magnitude of the drop size formed after the condensation shock will be predicted.

THEORETICAL ANALYSIS

Mathematical analysis of the flow stream across the condensation shock can be made by the use of four equations.

1. Energy

$$H_1 + \frac{V_1^2}{2gJ} = H_2 + \frac{V_2^2}{2gJ} \qquad (I)$$

2. Continuity

$$\frac{V_1}{v_1} = \frac{V_2}{v_2}, \text{ since } A_1 = A_2 \qquad (2)$$

3. Momentum

$$P_1 + \frac{V_1^2}{v_1 g} = P_2 + \frac{V_2^2}{v_2 g} \qquad (3)$$

or

$$V_2 = V_1 + \frac{g v_1}{V_1} (P_1 - P_2) \qquad (4)$$

4. $$P_{wv2} = f\ (T_2,\ r) \qquad (5)$$

The use of the fourth equation makes two analytical methods of approach possible.

(1) Either the drop size "r" can be assumed infinite, hence fixing the pressure rise due to the condensation shock, or

(2) The observed value of the pressure rise across

the shock may be used and the value of the drop size evaluated.

Since the second method of approach most nearly represents actual conditions, this will be followed. In addition, in order that actual conditions at the shock may be represented as closely as possible, the observed value of P_1/P_o at the position of the shock will be used in preference to the theoretical value.

The energy equation (I) may be written:

$$\frac{m_a\ (ha_1 - ha_2) + m_{wv1}h_{wv1} - m_{wv2}h_{wv2} - m^*h_{i2}}{m_a + m_{wv1}} = \frac{V_2^2 - V_1^2}{2gJ},$$

Simplifying the left hand side of the equation using:

$$m^* = m_{wv1} - m_{wv2}$$

$$\frac{m_a\ c_{pa}\ (T_1 - T_2) + m_{wv1}\ h_{wv1} - m_{wv2}\ h_{wv2} - (m_{wv1} - m_{wv2})h_{i2}}{m_a + m_{wv1}} =$$

$$\frac{V_2^2 - V_1^2}{2gJ}$$

Re-writing,

$$\frac{m_a\, c_{pa}\, (T_1 - T_2) + m_{wv1}\, (h_{wv1} - h_{i2}) - m_{wv2}\, (h_{wv2} - h_{i2})}{m_a + m_{wv1}}$$

$$= \frac{V_2^2 - V_1^2}{2gJ}$$

$$h_{i2} = h_{wv2} - h^*$$

$$h^* = h_{wv2} - h_{i2}$$

Substituting above

$$\frac{m_a\, c_{pa}(T_1 - T_2) + m_{wv1}\, (h_{wv1} - h_{wv2} + h^*) - m_{wv2}\, h^*}{m_a + m_{wv1}}$$

$$= \frac{V_2^2 - V_1^2}{2gJ}$$

$$\frac{m_a\, c_{pa}\, (T_1 - T_2) + m_{wv1}\, (h_{wv1} - h_{wv2}) + m^*\, (h^*)}{m_a + m_{wv1}}$$

$$= \frac{V_2^2 - V_1^2}{2gJ} \quad (6)$$

$$\frac{m_a\, c_{pa}\, (T_1 - T_2) + m_{wv1}\, c_{pwv}\, (T_1 - T_2) + m^*\, h^*}{m_a + m_{wv1}}$$

$$= \frac{V_2^2 - V_1^2}{2gJ} \quad (7)$$

Solving for m^*, and setting m_a = 1 lb.

$$m^* = \frac{-\frac{(1+w)(V_1^2 - V_2^2)}{2gJ} + 0.24(T_2 - T_1) + w(0.44)(T_2 - T_1)}{h^*} \quad (8)$$

Sample calculation of m^* from known pressure rise across shock.

Given:

P_o = _____ psi

w = _____ lb./lb.

T_o = _____ ^oR

$\frac{P_2 - P_1}{P_o}$ = _____ (measured)

x = _____ in. (measured)

$\frac{P_1}{P_o}$ = _____ (measured)

$P_1 = \frac{P_1}{P_o} \times P_o$ = _____ psi

$T_1 = T_o \left(\frac{P_1}{P_o}\right)^{\frac{k-1}{k}}$ = _____ ^oR

$P_{so} = \frac{w P_o}{.622\left(1 + \frac{w}{.622}\right)}$ = _____ psi

To find P_{s1} :

$P_{s1} = P_{so} \times \frac{P_1}{P_o}$ = _____ psi

From perfect gas relation using k = 1.4 and knowing P_1/P_o

M_1 = _____

$V_1 = 49\sqrt{T_1}\, M_1$ = _____ ft/sec

$v_1 = \frac{RT_1}{P_1 \times 144}$ = _____ cuft/lb

Using equation (4)

$V_2 = V_1 - \frac{g v_1}{V_1}(P_2 - P_1) \times 144$ = _____ ft/sec

$v_2 = \frac{V_2}{V_1} v_1$ = _____ ft^3/lb

The effect of the specific volume of the water vapor is not included as the correction is small.

$T_2 = \frac{P_2 v_2 \times 144}{R}$ = _____ ^oR

h^* obtained from Table 5, Reference (10).

From equation (8)

m^* = _____ lb/lb

It is of interest to note that regardless of whether h^* represents heat of fusion or of sublimation, there is little effect on the computed value of m^*. We chose

to make the calculation using both values of h^*, as it will be pointed out later that it is difficult to predict whether ice or water is formed in the shock.

This calculation was carried out for the eight curves on Figures V, VI, and VII. The details of this calculation are shown in the Appendix in Table VII. The first values of m^*, w_2, and P_{s2} were obtained using h^* equal to the heat of sublimation. For the second set of values, h^* equal to the heat of vaporization was used.

For this computation based on the known pressure rise across the shock it was found that the ratio $\frac{w_2}{w_1}$ increased as w_1 decreased. w_2 is defined as $w_1 - m^*$. This information is shown on Figure X. It is seen from this figure that with a known inlet specific humidity, the lbs. of water vapor per lb air after the shock can be predicted. The m^* used in the calculation of w_2 for Figure X was based upon h^* being the heat of sublimation.

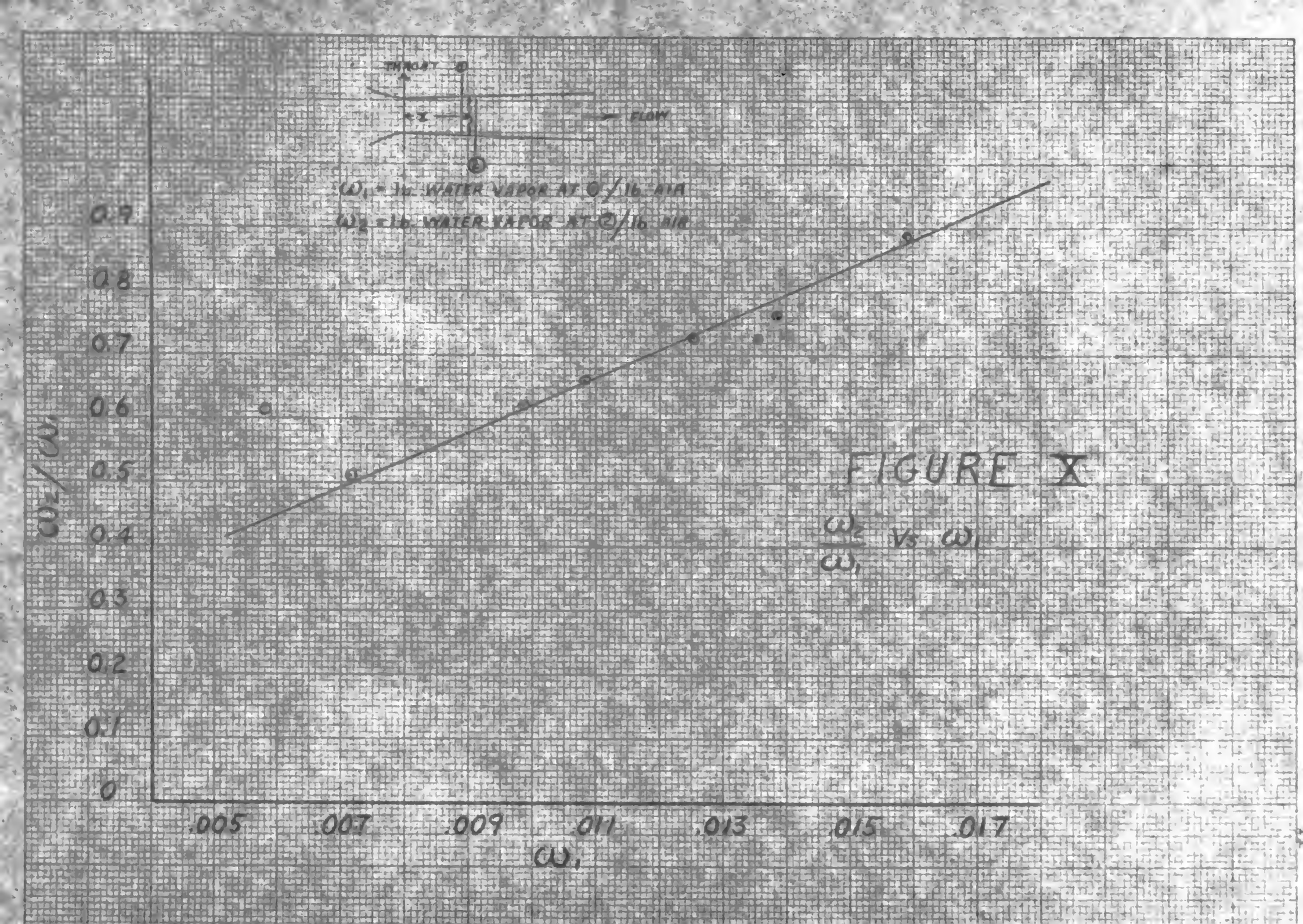

FIGURE X

$\frac{\omega_2}{\omega_1}$ Vs ω_1

It has been found that for steam, when expanding isentropically across the saturation line, that condensation does not occur until the Wilson Line is reached.

This line is located approximately 60 Btu below the saturation line on the Mollier diagram. A similar relation was sought for humid air expanding isentropically.

For a given w and T_o,

$$P_{so} = \frac{wP_o}{0.622}$$

Selecting a pressure ratio P/P_o,

$$P_s = P_{so} \left(\frac{P}{P_o}\right)$$

From the perfect gas relation the temperature of the mixture corresponding to $\frac{P}{P_o}$ is

$$T = T_o \left(\frac{P}{P_o}\right)^{\frac{k-1}{k}}$$

From the calculated T and reference (10), the saturation pressure, P_{sat}, for equilibrium conditions can be computed. A cut and try process in which various values of P/P_o are assumed is then used to make $P_s = P_{sat}$ giving the temperature at which the air becomes saturated. The results of such a computation are shown on Figure XI. Using computed values of T_1, the following results

were obtained.

TABLE II

W	T_{sat}	T_1	$T_{sat} - T_1$
.00581	496	384	112
.00714	501	388	113
.00982	510	400	110
.01082	514	405	109
.01254	520	411	109
.01358	522	412	110
.01384	523	416	107
.01588	528	425	103

The results indicate that the condensation shock occurs at $T_{sat} - T_1 \cong 110^{\circ}F$. There appears to be a slight trend for the temperature difference to decrease with increasing specific humidity.

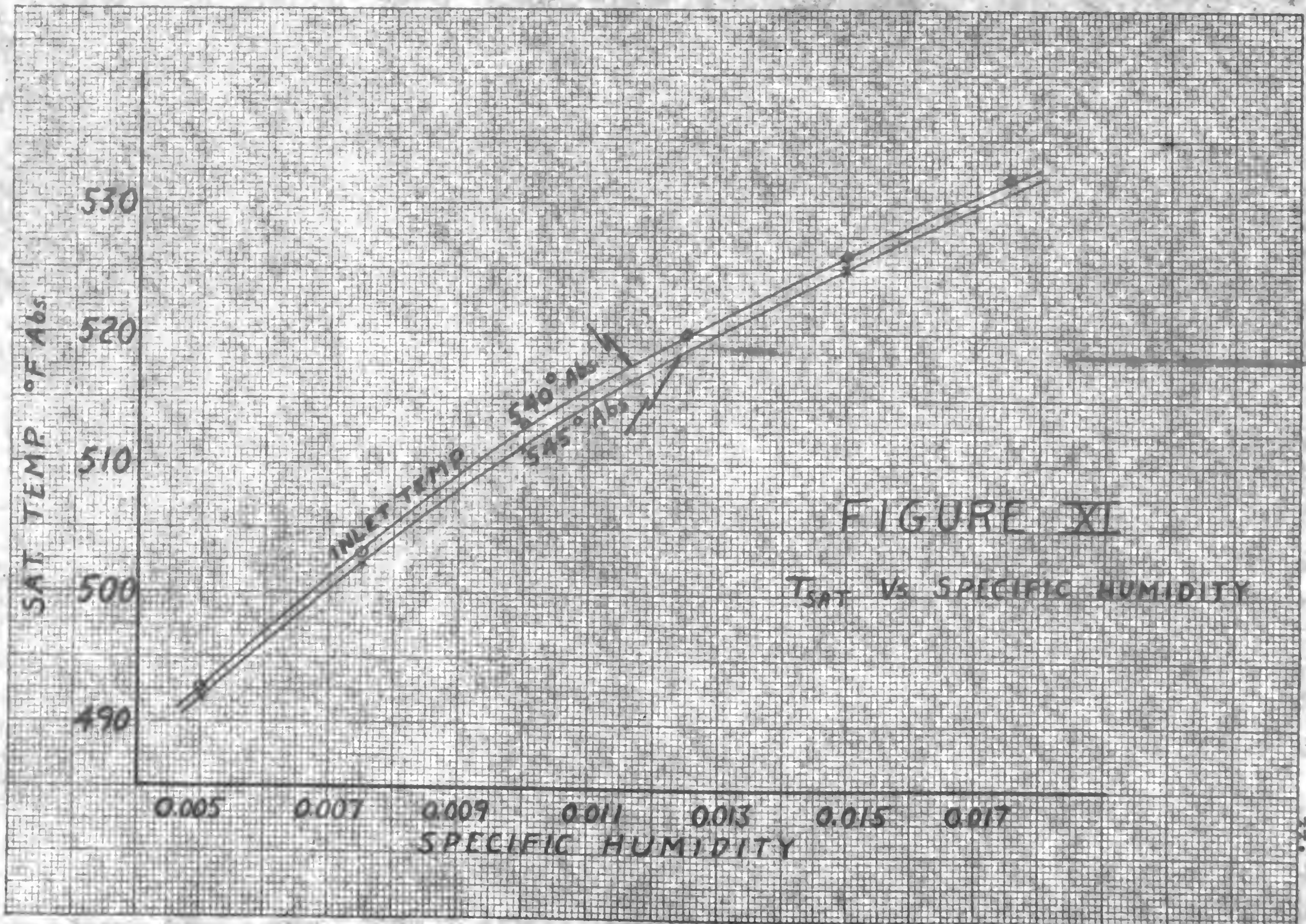

FIGURE XI

T_{SAT} Vs SPECIFIC HUMIDITY

We define $w_2 = w_1 - m^*$ (9)

then, $w_2 = 0.622 \frac{P_{s2}}{P_2}$ (10)

or, $P_{s2} = \frac{w_2 P_2 x \blacksquare}{0.622}$ psi (11)

Values of P_{s2} were computed for the eight runs for which m^* was computed. It was found upon comparing P_{s2} computed from formula (11), that P_{s2} was much greater than the saturation pressure for equilibrium conditions corresponding to the temperature T_2.

Now we will review the events occuring in the flow of the humid air through the nozzle. At the nozzle inlet the water vapor in the air is in a superheated state. The mixture of water vapor and air is expanded isentropically through the nozzle and at a temperature of about 110 degrees below the temperature at which condensation should have occured, some of the water vapor condenses out. As mentioned above, the vapor pressure after the shock is greater than the equilibrium vapor pressure at that temperature. The vapor pressure under stable conditions is that corresponding to vapor in equilibrium with drops of infinite radius. The Von-Helmholtz relation * shows that if the pressure

*Reference (11), pages 434 - 437

of the water vapor is greater than the saturation pressure under equilibruim conditions, then the water vapor is in equilibruim with drops of less than infinite radius.

By means of the Von-Helmholtz equation, (see Appendix pp. 62), Figure XII, which follows, was drawn. Figure XII shows, for various drop sizes, the pressure of the water vapor in equilibruim with those drops for a given temperature. Calculated points from the eight runs which were calculated in detail (Table VII) are shown on Figure XII. These points are plotted using T_2 and P_{s2} as arguments. The circled points correspond to P_{s2} computed on the basis that water forms and the "x" points correspond to P_{s2} computed on the basis that ice forms. The four low specific humidity points lie at a pressure below the triple point pressure of 0.0888 psi. Under stable conditions, ice would be formed in the shock at these low pressures. The vapor pressures of the four high humidity points lie above the triple point pressure and probably water droplets would form in the shock. However, it is difficult to predict in this metastable state whether ice or water droplets form. For the four high humidity runs, it appears that a drop size of about 3×10^{-9} feet is formed in the shock. It is possible that

FIGURE XII

PLOT SHOWING THE SIZE OF WATER DROPLETS FORMED IN A CONDENSATION SHOCK

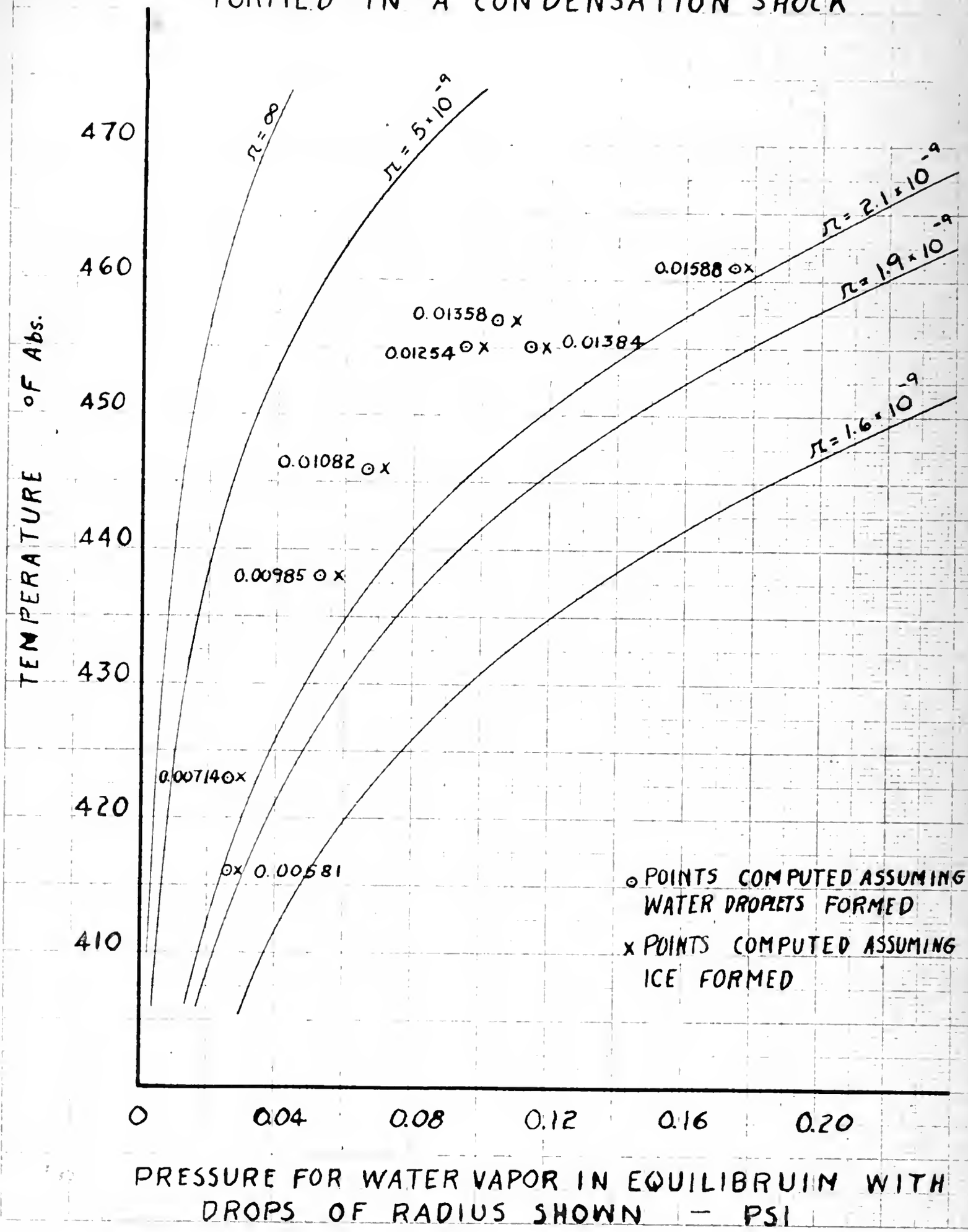

a metastable state of subcooled water exists below the triple point pressure. If this is true, it appears from Figure XII that for all specific humidities the drop size forming in the shock is of a radius of about 3×10^{-9} feet. Because of our inability to predict the exact nature of this phenomena, both the circled and "x" points are shown.

It must be mentioned that in the computation of drop size it was found that the various reliable authorities give an appreciable variation in the values of $P_{s\infty}$ at temperatures below $32^{\circ}F$. These discrepencies increase with decreasing temperatures. Also values of surface tension are not definitely known at these low temperatures.

In conclusion, it is obvious that further exploration of this subject is necessary in order to present a complete picture. However, it is hoped that the results of our experiments will contribute to the knowledge of this subject.

RECOMMENDATIONS

(1) In preference to the conventional two dimensional nozzle, it would be better to use a half nozzle contour with a sliding straight wall section fitted with a pressure tap and a micrometer screw for accurate longitudinal measurement of the position at which the pressure is measured.

(2) More accurate humidity measurements are desirable. Chemical methods can give any desired degree of accuracy.

(3) It is desirable to cover a wider range of inlet temperatures and specific humidities.

(4) Verify the proposed correlation that a plot of area ratio against specific humidity for a given inlet temperature will determine the position of the condensation shock for nozzles of various contours.

APPENDIX

		Page
Table III	- Original Data	51
Table IV	- Original Data	56
Table V	- Original Data	58
Table VI	- Data of nozzle areas and area ratios	59
Figure XIII	- Area and area ratio Vs distance along the nozzle	60
Table VII	- Detailed calculation across the condensation shock	61
Table VIII	- Calculation of vapor pressure of water vapor in thermal equilibrium with drops of various radii.	62

TABLE III

Run	1	2	3	4	5	UNITS
% Rel.Hum.	100	36.8	77	75.5	65	^{o}F
D.B.	90.8	82.9	80.4	80.8	82.7	^{o}F
W.B.	90.8	79.6	74.9	74.7	73.4	^{o}F
P_o	75.7	75.70	75.7	75.65	75.65	cm. Hg.
P_{10}	42.55	40.70	40.45	40.25	40.20	"
P_9	36.95	35.90	35.65	35.45	33.85	"
P_8	32.35	32.30	32.30	32.40	32.25	"
P_7	25.20	24.30	23.90	23.75	23.55	"
P_2	12.80	12.00	11.70	11.60	11.35	"
ω					.01588	lbs. w. v./ lbs. air
Picture	Yes	Yes	Yes	Yes	Yes	
P_{10}/P_o					.532	
P_9/P_o					.448	
P_8/P_o					.427	
P_7/P_o					.312	
P_2/P_o					.150	
x^*					.41	
x^*/t					.84	

TABLE III (Cont.'d)

Run	6	7	8	9	10	11
% R.H.	63	61	56	51	51	50
D.B.	78	83.2	84.3	84.9	78.2	78.3
W.B.	69	73.0	72.4	71.4	65.8	65.5
P_o	76.15	75.65	75.6	75.6	76.15	76.15
P_{10}	40.20	40.15	40.15	40.05	40.20	40.10
P_9	33.20	33.45	32.60	32.30	32.30	32.25
P_8	30.95	32.25	32.35	32.25	30.85	30.90
P_7	22.95	23.50	23.20	22.95	22.10	22.05
P_2	11.15	11.30	11.20	11.10	10.70	10.65
ω	.01313	.01513	.01439	.01328	.01070	.01053
Picture	Yes	Yes	Yes	Yes	Yes	Yes
P_{10}/P_o	.528	.532	.532	.530	.528	.526
P_9/P_o	.436	.442	.431	.427	.424	.424
P_8/P_o	.407	.427	.428	.427	.405	.406
P_7/P_o	.302	.311	.307	.304	.290	.290
P_2/P_o	.146	.1496	.148	.147	.141	.141
x^*	.47	.43	.49	.53	.57	
x^*/t	.96	.88	1.00	1.08	1.16	

TABLE III (Cont.'d)

Run	12	13	14	15	16	17
% R.H.	47	46	44	43.6	42	42
D.B.	85.7	79	80.5	86	84.6	82.2
W.B.	70.8	64.8	65.7	69.8	68.2	66.2
P_o	75.40	76.05	75.95	75.30	75.25	75.75
P_{10}	39.95	40.05	40.00	39.85	39.95	39.95
P_9	32.15	32.20	32.15	32.00	32.00	32.05
P_8	32.30	30.30	30.25	31.00	30.40	28.60
P_7	22.60	21.85	21.80	22.05	22.00	21.55
P_2	10.90	10.55	10.55	10.65	10.60	10.45
ω	.01265	.00992	.00998	.01190	.01092	.01011
Picture	Yes	Yes	No	Yes	Yes	Yes
P_{10}/P_o	.530	.527	.527	.530	.531	.527
P_9/P_o	.426	.424	.423	.425	.425	.423
P_8/P_o	.428	.398	.398	.411	.404	.378
P_7/P_o	.300	.287	.287	.292	.292	.284
P_2/P_o	.145	.139	.139	.1415	.141	.138
x^*	.55	.59		.60	.60	.65
x^*/t	1.12	1.20		1.22	1.22	1.33

TABLE III (Cont.'d)

Run	18	19	20	21	22	23
% R.H.	40	39.5	39	37	36	34
D.B.	83.5	83.0	84.9	84.2	86	87.2
W.B.	66.5	66.2	67.1	66.0	66.8	66.9
P_o	75.75	75.15	75.75	75.75	75.65	75.65
P_{10}	39.90	39.75	39.90	39.90	39.90	39.75
P_9	32.05	31.95	32.05	32.05	32.05	31.90
P_8	28.40	30.05	28.60	28.60	27.90	26.45
P_7	21.60	21.65	21.65	21.65	21.75	21.70
P_2	10.45	10.40	10.50	10.50	10.50	10.40
ω	.01004	.00975	.01027	.00951	.00982	.00964
Picture	Yes	No	Yes	Yes	Yes	Yes
P_{10}/P_o	.527	.530	.527	.527	.526	.526
P_9/P_o	.423	.425	.423	.423	.424	.422
P_8/P_o	.378	.400	.378	.378	.369	.350
P_7/P_o	.285	.288	.286	.286	.288	.287
P_2/P_o	.138	.1385	.139	.139	.139	.138
x^*	.66		.65	.65	.65	.75
x^*/t	1.35		1.33	1.33	1.33	1.53

TABLE III (Cont.'d)

Run	24	25	26
% R.H.	30.5	27.5	22
D.B.	88.7	90.2	92.4
W.B.	66.5	66.7	66.5
P_o	75.25	75.20	75.0
P_{10}	39.65	39.65	39.50
P_9	31.80	31.80	31.65
P_8	25.30	24.95	24.45
P_7	21.85	21.85	21.40
P_2	10.35	10.35	10.25
ω	.00913	.00856	.00741
Picture	Yes	Yes	Yes
P_{10}/P_o	.527	.527	.526
P_9/P_o	.423	.423	.422
P_8/P_o	.336	.332	.326
P_7/P_o	.290	.290	.286
P_2/P_o	.138	.138	.136
x^*	.76	.80	.88
x^*/t	1.55	1.63	1.8

TABLE IV

Run	1	2	3	4	5	UNITS
% Rel.Hum.	24.0	27.5	34.5	37.5	41.0	°F
D.B.	82.4	84.5	85.4	85.5	85.0	°F
W.B.	59.8	62.9	65.8	67.0	68.0	°F
P_o	74.95	75.05	75.40	75.60	75.70	cm. Hg.
P_{10}	40.00	40.1	40.25	40.40	40.50	"
$P_{9\frac{1}{2}}$	37.95	38.00	38.20	38.30	38.40	"
P_9	32.70	32.70	32.85	32.95	33.00	"
$P_{8\frac{1}{2}}$	27.20	27.30	27.50	27.90	28.65	"
P_8*	31.00	31.25	32.40	33.60	34.60	"
$P_{7\frac{1}{2}}$	22.85	23.95	25.15	2600	26.50	"
P_7	21.10	21.80	21.75	22.00	22.25	"
P_6	16.80	17.30	18.15	18.70	18.06	"
P_4*	14.30	14.65	15.10	15.40	15.06	"
P_2	9.90	10.15	10.35	10.55	10.70	"
P_{10}/P_o	.534	.535	.534	.535	.535	
$P_{9\frac{1}{2}}/P_o$	.505	.506	.506	.507	.507	
P_9/P_o	.436	.436	.435	.436	.436	
$P_{8\frac{1}{2}}/P_o$	.363	.364	.365	.369	.378	
$P_{7\frac{1}{2}}/P_o$	.305	.318	.333	.344	.350	
P_7/P_o	.282	.290	.288	.291	.294	
P_6/P_o	.224	.231	.241	.248	.246	
P_2/P_o	.120	.135	.137	.140	.141	
ω	.00581	.00714	.00923	.00997	.01082	lbs. w. v./ lbs. air

* Values not used

TABLE IV (Cont.'d)

Run	6	7	8	9	10
% R.H.	46.0	49.0	55.5	58.0	98.0
D.B.	83.5	83.6	82.8	82.0	87.0
W.B.	68.5	69.4	70.6	70.8	86.5
P_o	75.80	75.90	76.10	76.10	76.10
P_{10}	40.60	40.65	40.85	40.70	41.85
$P_{9\frac{1}{2}}$	38.50	38.55	38.55	38.60	40.55
P_9	33.10	33.15	33.35	33.60	37.30
$P_{8\frac{1}{2}}$	30.20	31.10	32.90	34.60	34.60
P_8*	35.80	36.55	39.30	40.50	38.30
$P_{7\frac{1}{2}}$	26.90	27.30	27.05	27.00	28.80
P_7	22.65	22.80	23.25	23.30	25.10
P_6	18.70	18.80	19.05	19.15	21.30
P_4*	15.85	15.95	16.05	16.20	17.60
P_2	10.90	10.95	11.10	11.10	12.70
P_{10}/P_o	.535	.536	.537	.535	.550
$P_{9\frac{1}{2}}/P_o$	.508	.508	.507	.507	.534
P_9/P_o	.436	.436	.438	.441	.490
$P_{8\frac{1}{2}}/P_o$	.398	.410	.432	.455	.455
$P_{7\frac{1}{2}}/P_o$	.354	.360	.356	.355	.379
P_7/P_o	.299	.300	.306	.306	.330
P_6/P_o	.246	.248	.250	.252	.280
P_2/P_o	.144	.144	.146	.146	.167
ω	.01254	.01233	.01358	.01384	.02764

* Values not used

TABLE V

Run	% Rel.Hum.	ω	D.B.	W.B.	x^*	x^*/t
1	63.0	.0107	72.4	63.8	.49	1.00
2	57	.0099	73.4	63.2	.53	1.08
3	50	.0088	73.5	61.4	.57	1.16
4	46	.0083	74.2	61.0	.59	1.20
5	45	.0080	74.0	60.4	.60	1.225
6	42.5	.0076	74.5	60.0	.61	1.245
7	41	.0075	74.6	59.8	.62	1.265
8	36.5	.0070	75.7	59.4	.65	1.327
9	31	.00645	76.6	59.0	.69	1.410
10	30	.00585	77.6	58.5	.73	1.490
11	30	.00610	78.2	59.0	.74	1.510
12	28.5	.00600	78.7	59.0	.79	1.610

TABLE VI

DATA OF NOZZLE AREAS AND AREA RATIOS

Stations are spaced 0.4 inches apart (see Figure XIII following). The nozzle is 0.50 inches thick.

Station	Area, $in.^2$	A/A_T
2	.442	1.804
3	.4135	1.690
4	.384	1.567
5	.356	1.453
6	.328	1.340
7	.2975	1.214
8	.271	1.107
9	.248	1.012
10(Throat)	.2455	1.000
11	.2455	1.002
12	.246	1.004
13	.279	1.139
14	.335	1.37

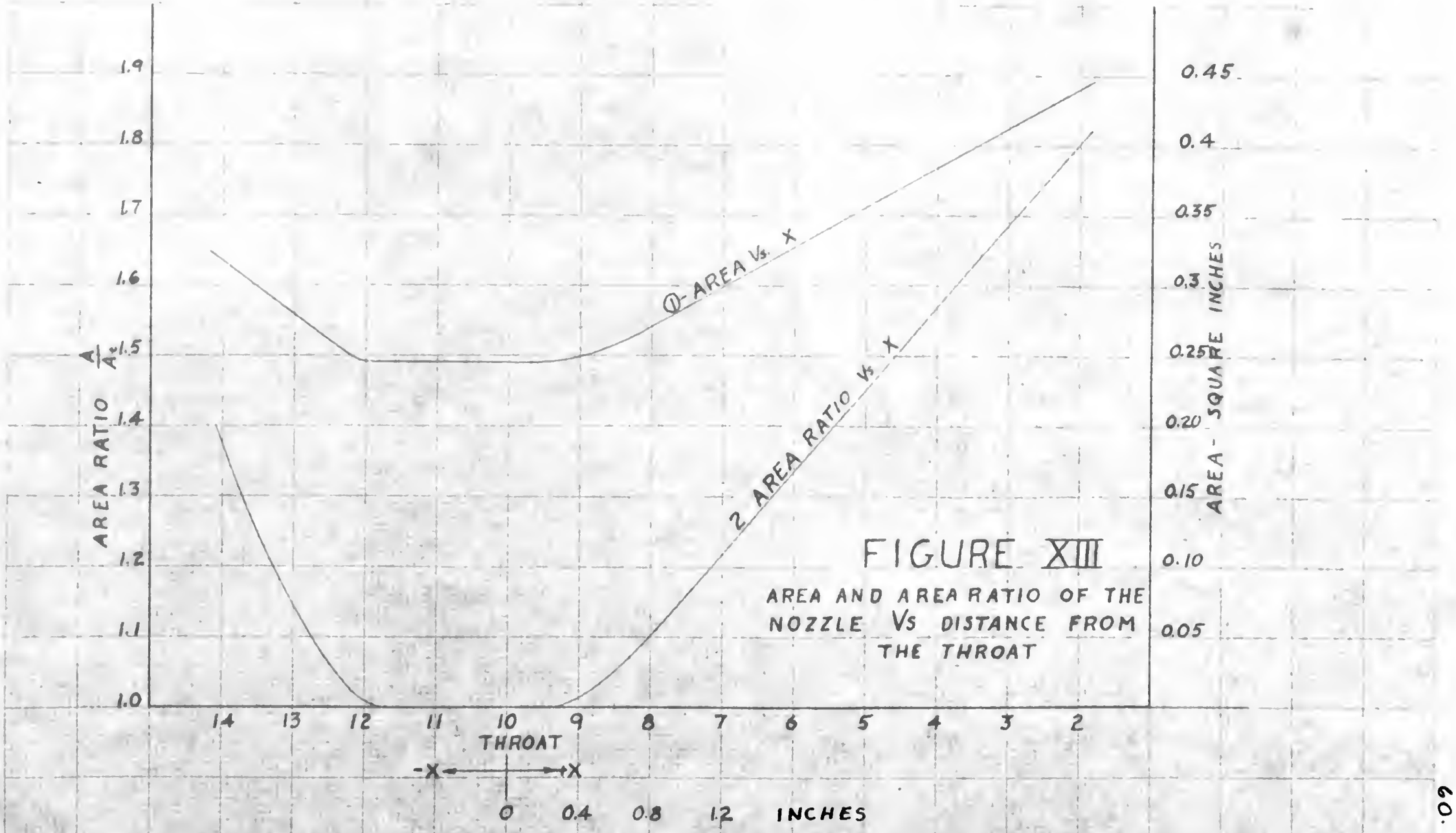

FIGURE XIII

AREA AND AREA RATIO OF THE NOZZLE Vs DISTANCE FROM THE THROAT

TABLE VII
DETAIL CALCULATION ACROSS CONDENSATION SHOCK

CURVE NO	1	2	3	4	5	6	7	8	
P_o	74.95	75.05	75.65	75.7	75.8	76.1	76.1	75.65	CM. Hg
$P_o \cdot 0.1934$	14.50	14.50	14.64	14.65	14.66	14.70	14.70	14.64	Psi
ω	.00581	.00714	.00985	.01082	.01254	.01358	.01384	.01588	$\frac{\text{lb water vapor}}{\text{lb air}}$
T_o	542.4	544.5	546	545	543.5	542.8	542	542.7	°R
t_o	82.4	84.5	86.0	85.0	83.5	82.8	82.0	82.7	°F
WB	59.8	62.9	66.8	68.0	68.5	70.6	70.8	73.4	°F
$(P_2 - P_1)/P_o$	0.044	0.051	0.062	0.073	0.092	0.094	0.082	0.106	FROM FIG VIII
$P_2 - P_1$	0.638	0.74	0.907	1.07	1.348	1.380	1.205	1.552	Psi
X	0.83	0.81	0.70	0.65	0.593	0.550	0.515	0.430	IN.
P_1/P_o	0.300	0.307	0.340	0.352	0.375	0.382	0.395	0.425	FIG 9 XI. VIII
$(P_1/P_o)^{0.286}$	0.709	0.713	0.734	0.742	0.756	0.760	0.767	0.783	
$T_1 = T_o (P_1/P_o)^{0.286}$	384	388	400	405	411	412	416	425	
P_1	4.35	4.45	4.98	5.15	5.50	5.61	5.80	6.22	Psi
P_2	4.99	5.19	5.88	6.22	6.85	6.99	7.01	7.77	Psi
$P_{s_o} = \frac{\omega P_o}{.622(1+\omega/.622)}$	0.134	0.165	0.228	0.251	0.289	0.312	0.320	0.364	Psi
$P_{s_1} = P_{s_o} \cdot P_1/P_o$	0.0402	0.0506	0.0775	0.088	0.1085	0.120	0.1265	0.1650	Psi
M_1	1.433	1.417	1.343	1.318	1.271	1.257	1.233	1.177	PERFECT GAS REL
$V_1 = 49\sqrt{T_1} \cdot M_1$	1378	1367	1318	1300	1262	1250	1232	1189	FT/sec
$V_1 - V_2$	70	81	95	111	137	139	121	152	FT/sec
$v_1 = T_1 \cdot 37/P_1$	32.6	32.2	29.7	29.1	27.6	27.2	26.6	25.2	CU FT/lb
$V_2 = V_1 - \frac{32}{V_1}(P_2 - P_1)144$	1308	1286	1223	1189	1125	1111	1111	1037	FT/sec
$v_2 = \frac{V_2}{V_1} \cdot v_1$	30.9	30.2	27.6	26.6	24.6	24.2	24.0	22.0	CU FT/lb
$T_2 = P_2 v_2 \cdot 2.7$	416	423	438	446	455	457	455	461	°R
$(V_1 - V_2)(V_1 + V_2)/50000$	3.76	4.29	4.82	5.52	6.55	6.55	5.66	6.77	Btu/lb
h^*	1221.2	1221.2	1221.2	1221.2	1221.2	1221.2	1221.2	1221.2	Btu/lb
$T_2 - T_1$	-32	35	38	41	44	45	39	36	°F
$\frac{(1+\omega)(V_1^2 - V_2^2)}{50000}$	-5.02	-4.16	-4.75	-5.57	-6.60	-6.48	-5.60	-6.80	Btu/lb
$.024(T_2 - T_1)$	7.68	8.40	9.12	9.84	10.55	10.80	9.35	8.65	Btu/lb
$0.44\omega(T_2 - T_1)$	0.08	0.11	0.16	0.20	0.24	0.27	0.24	0.25	Btu/lb
Σ	2.74	4.35	4.53	4.47	4.19	4.59	3.99	2.10	Btu/lb
SUBLIMATION $m^* = \frac{\Sigma}{h^*}$	.00224	.00356	.00371	.00367	.00343	.00376	.00327	.00172	$\frac{\text{lb water}}{\text{lb air}}$
SUBLIMATION $\omega_2 = \omega_1 - m^*$	.00357	.00358	.00614	.00715	.00911	.00982	.01057	.01416	$\frac{\text{lb water vapor}}{\text{lb air}}$
P_{s_2}	.0287	.0299	.0581	.0715	.1006	.1100	.1190	.178	Psi
VAPORIZATION h^*	1077	1077	1077	1077	1077	1077	1077	1077	Btu/lb
VAPORIZATION m^*	.00255	.00405	.00422	.00416	.00390	.00427	.00372	.00196	lb/lb
VAPORIZATION $\omega_3 = \omega_1 - m^*$	.00326	.00302	.00563	.00666	.00864	.00931	.01012	.01392	lb/lb
P_{s_2}	.0262	.0259	.0533	.0666	.0952	.1045	.1141	.1743	Psi

The calculation of the vapor pressure of water vapor in thermal equilibrium with drops of various radii for various temperatures:

$$\text{Ln}\ \frac{P_{sr}}{P_{s\infty}} = \frac{2\sigma v^l}{rRT}$$

Where R = 85.8 and σ is the surface tension in dynes/cm. given by:

$$\sigma^{*} = 75.64 - 0.1391t - .0003t^2 \qquad (t \text{ in } {}^{o}C)$$

$P_{s\infty}$ is given by the equation below:

$$\log_{10} P^{**}_{s\infty} = 21.075 - \frac{2903.39}{T} - 4.71734 \log_{10} T$$

Where T is expressed in ^{o}Kelvin.

$P_{s\infty}$ is in psi.

---

* Reference (11) pp.447
** Reference (7) pp.569

TABLE VIII

T	$\sigma \times 10^3$	v^1	$P_{s\infty}$	$r=1.6\times10^{-9}$		$r=1.9\times10^{-9}$	
				$P_{sr}/P_{s\infty}$	P_{sr}	$P_{sr}/P_{s\infty}$	P_{sr}
(°F)	lb/ft	cuft/lb	psi				
470	5.29	.160	.0354	13.8	0.488	9.1	.322
460	5.34	.160	.0224	15.01	0.336	9.8	.220
450	5.39	.160	.0139	16.25	0.226	10.45	.145
440	5.43	.160	.00841	17.80	0.150	11.30	.095
430	5.48	.160	.00496	19.50	0.0966	12.20	.0605
420	5.52	.160	.00284	21.40	0.0608	13.20	.0375
410	5.56	.160	.00158	23.50	0.0372	14.30	.0226

T	$r=2.1\times10^{-9}$		$r=5\times10^{-9}$	
	$P_{sr}/P_{s\infty}$	P_{sr}	$P_{sr}/P_{s\infty}$	P_{sr}
470	7.40	.264	2.32	.082
460	7.88	.1766	2.38	.0533
450	8.40	.1168	2.44	.0340
440	8.98	.0755	2.51	.0211
430	9.65	.0478	2.58	.0128
420	10.35	.0294	2.66	.00755
410	11.15	.0176	2.74	.00433

BIBLIOGRAPHY

1. J. I. Yellott, Jr., "Supersaturated Steam", A.S.M.E. Transactions, Vol. 56, 1934, pp. 411-430.

2. J. I. Yellott, Jr., and C. K. Holland, "The Condensation of Flowing Steam", A.S.M.E. Transactions, Vol. 59, 1937, pp. 171-183.

3. R. Hermann, "Condensation Shock Waves in Supersonic Wind Tunnel Nozzles", Luftfahrtforsehung, Vol. 19, No. 6, June 20, 1942, pp. 201-209.

4. K. Oswatitsch, "Condensation Phenomena in Supersonic Nozzles", Z.A.M.M., Vol. 22, No. 1, February 1942, pp. 1-14.

5. A.M. Binnie and M.W. Woods, "The Pressure Distribution in a Converging-Diverging Steam Nozzle", Proc. Inst. Mech. Engrs., Vol. 138, 1938, pp. 229-231.

6. L. A. DeFrate, "Investigation of Supersonic Flow in Nozzles and Tubes by the Schlieren Method", Master's Thesis, MIT, 1943. (M.E. Department).

7. C.F. Powell, Proceedings of the Royal Society, Vol. 114 (A), 1928, Pp. 553.

8. O.T. Zimmerman and Irvin Lavine, "Psychrometric Tables and Charts" Industrial Research Service, Dover, New Hampshire.

9. U.S. Dept. of Commerce Bulletin, W-B 235, U.S. Government Printing Office 1941.

10. J.H. Keenan and F. G. Keyes, Thermodynamic Properties of Steam, New York, 1944.

11. J.H. Keenan, Thermodynamics, New York, 1941.